

**DESIGN AND CHARACTERIZATION OF TARGETED DRUG DELIVERY  
OF CARBON QUANTUM DOTS FROM A NATURAL PRECURSOR  
FOR CANCER TREATMENT**

A Dissertation submitted to  
**THE TAMIL NADU Dr. M.G.R. MEDICAL UNIVERSITY  
CHENNAI – 600 032**

In partial fulfillment of the requirements for the award of the Degree of  
**MASTER OF PHARMACY**  
IN  
**BRANCH- I - PHARMACEUTICS**

Submitted by  
**MOHAMMED WASEEM .A**  
REGISTRATION No: 261810152

Under the guidance of  
**DR. M.A. AMUTHA GNANA ARASI, M.Pharm., Ph.D.**  
Department of Pharmaceutics



**COLLEGE OF PHARMACY  
SRI RAMAKRISHNA INSTITUTE OF PARAMEDICAL SCIENCES  
COIMBATORE – 641044**

**MARCH 2020**

## ACKNOWLEDGEMENT

I thank **God Almighty** for the wisdom and perseverance that had been bestowed upon me during this research project. It's because of His grace I was able to successfully complete my project.

Words are insufficient to express my gratitude and respect towards my guide, **Dr. M.A. Amutha Gnana Arasi, M. Pharm., (Ph.D.)**, Assistant Professor, Department of Pharmaceutics, who mentored me in this innovative pharmaceutical research work at every stage and took great care in making me proceed on the right path, through her valuable suggestions and inspirations.

My sincere gratitude to our beloved Principal **Dr. T.K.Ravi, M.Pharm., Ph.D., FAGE.**, for supporting and providing every need from time to time to complete this work successfully.

I express my deep sense of gratitude and indebtedness to **Dr. M. Gopal Rao, M.Pharm., Ph.D.**, Vice principal and Head, Department of Pharmaceutics, for his valuable suggestions and support during this project.

I express my sincere thanks to our beloved Managing Trustee **Thiru. Lakshmi Narayana Swamy, Managing Trustee, M/s. SNR Sons Charitable Trust, Coimbatore** for providing all the facilities to carry out this work.

I owe my profound gratitude to **Dr. M. Gandhimathi, M.Pharm., Ph.D.**, for helping me to carry out the analytical studies and also for being a beacon of wisdom in resolving any challenges I faced during the course of work.

My sincere thanks to my dear teachers **Dr. S. Krishnan M.Pharm., Ph.D.**, **Dr.K. Muthuswamy, M.Pharm., Ph.D.**, **Dr.J. Bhagyalakshmi, M. Pharm., Ph.D.**, **Dr. A.S. Manjuladevi M.Pharm., Ph.D.**, and **Dr. R.M. Akila M.Pharm., Ph.D.** for their moral support and guidance during the course of work.

I would also like to thank **Dr. Venkataswamy, M.Sc., Ph.D., Mr.S. Muruganandham, Mrs. Dhanalaxmi** and Mrs. **Kalaivani** for their kind co-operation during this work.

I remain greatly indebted to my parents **Mr. Abdul Muthalif and Mrs. Jareena** and my brother **Mr. Mohammed Shameem** for their precious love, affection and moral support which kept me on high spirits and are also the backbone for all successful endeavors in my life.

Words cannot express my gratitude to my friends **Ansu, Sai, Ann Maria, Tresa, Ajmal, Ajin, Kathiravan, Dhanapal, Dhanya, Anvitha, Manikandan, Surendran** for their support, cooperation and inspiration during the course of my work.

I wish to extend my sincere thanks to all my batchmates, seniors and juniors who directly or indirectly helped me during my work.

I express my gratitude to all my dear teachers, friends and relatives for their support during my work.

I wish to thank **Saraswathi Computer Centre** for framing project work in a beautiful manner.

**Mohammed Waseem**

## CONTENTS

Sl. No.	TITLES	PAGE No.
	LIST OF ABBREVIATIONS	
	LIST OF TABLES	
	LIST OF FIGURES	
1	INTRODUCTION	1
2	LITERATURE REVIEW	8
3	AIM AND OBJECTIVE	22
4	PLAN OF WORK	23
5	MATERIALS AND EQUIPMENTS	24
6	DRUG PROFILE	25
7	PLANT PROFILE	28
7	CROSS LINKING AGENT PROFILE	30
8	EXPEERIMENTAL METHODS	31
9	RESULT AND DISCUSSION	36
10	SUMMARY AND CONCLUSION	58
	BIBLIOGRAPHY	

## Abbreviation

---

### ABBREVIATIONS

CQDs	-	carbon quantum dots
SNB	-	sorafenib
FT-IR	-	Fourier Transform Infrared
UV	-	UltraViolet
SEM	-	Scanning Electron Microscopy
TPP	-	Sodium Tri poly phosphoric
RM	-	Raman spectrum
cm	-	centimetre
<i>et al.</i>	-	and others
g	-	gram(s)
hrs	-	hour(s)
min(s)	-	minutes
mg	-	milligrams
ml	-	millilitre
nm	-	nanometer
µg	-	micrograms
$\lambda_{\max}$	-	absorption maxima
mV	-	millivolt
KBr	-	Potassium Bromide
PDI	-	Poly Dispersity Index
$r^2$	-	Regression Value
vs.	-	Versus

## LIST OF TABLES

<b>Table no.</b>	<b>List of Tables</b>	<b>Page No.</b>
1	Average Quantum yields of CQDs	39
2	Interpretation of FTIR spectrum of prepared CQDS	42
3	Interpretation of Mass spectrum of prepared CQDs	44
4	Elementary of FTIR spectrum of prepared CQDS	45
5	Solubility evaluation of Sorafinib	46
6	Calibration concentration of Sorafinib	47
7	Formulation of sorafinib COQ-Dot Conjugates.	48
8	Encapsulation efficiency and Percentage yield of sorafinib COQ-Dot conjugate	49
9	FTIR interpretation of sorafinib	50
10	FTIR interpretation of polymer	51
11	FTIR interpretation of sorafinib COQ-Dot conjugate	52
12	<i>In-vitro</i> drug release profile of sorafinib COQ-Dot conjugate (SF1-SF5)	53

## LIST OF FIGURES

S. No	Title	Page No.
1	Emission spectrum of carbon dot	37
2	The CQDs deposited on invert fluorescence in uv chamber and scanned between 365-700nm	37
3	Emission spectrum (a) quinenine sulphate (b) carbon dots	38
4	Calibration plot of (A) Quinine Sulphate (B) CQDs	38
5	Particle size distribution of CQDs	40
6	Particle size distribution of CQDs	41
7	HRTEM of CQDs	41
8	FTIR spectrum of CQDs	42
9	Raman spectrum of CQDs	43
10	Elementary analysis of prepared CQDs	44
11	Confocal fluorescence imaging of prepared CQDs	45
12	UV/Visible spectrum of Sorfinib	46
13	Calibration curve of Sorfinib	47
14	UV Absorbance spectrum of formulated sorafinib COQ-Dot conjugate	47
15	Sorafinib IR Spectrum	50
16	Cross linking agent TPP IR Spectrum	51
17	Formulation sorafinib COQ-Dot conjugate IR Spectrum	51
18	<i>In vitro</i> drug release profile of sorafinib COQ-DotS formulations (F1-F5)	53
19	Cytotoxicity of bare C-dots, bare sorafinib(Standard), and Sorafi@C-dots conjugate on SHSY5H cell lines	54
20	Results from confocal fluorescence imaging (458 nm excitation) of (A) sorafinib (B) functionalized Sorafinib COQ-Dot conjugate carbon dots internalized SHSY5H in (incubation for 48 h).	55

<b>S. No</b>	<b>Title</b>	<b>Page No.</b>
21	Cytotoxicity of bare C-dots, bare sorafinib(Standard), and Sorafi@C-dots conjugate on MDA-MB 231 cell lines	56
22	Results from confocal fluorescence imaging (458 nm excitation) of (A) sorafinib (B) functionalized sorafinib COQ-Dot conjugate carbon dots internalized MDAMB231 in (incubation for 48 h)	56
23	Results from confocal fluorescence imaging (458 nm excitation) of carbon dots internalized SHSY5H cells in (incubation for 48 h).	57
24	24 Results from confocal fluorescence imaging (458 nm excitation) of carbon dots internalized MDA MB 231 cells in (incubation for 48 h).	57

## INTRODUCTION

Targeted drug delivery, localised disease treatment, and personalised cure are the ultimate goals in modern medicine. Such a development relies on precise biochemical fundamental understandings and equally importantly, observable biochemical activity reporters. In current cancer treatment, chemotherapy is still regarded as the most effective method, which as widely known, causes significant side effects to patients, because of their non-discriminating destructive impact on both cancer and normal cells<sup>[1][5]</sup>. The significant challenge in cancer chemotherapy and most complex diseases is to understand the drug distribution within the 30 organs and to devise a selective drug release system targeted at cancer cells. Therefore, developing sophisticated strategies to achieve both targeted and traceable anti-cancer drug delivery is of critical importance <sup>[6][7]</sup>. Recent years have seen increased activities in developing 50 multifunctional nanomaterials that can enable bioimaging, disease detection and drug delivery simultaneously. Various nanoparticles (NPs) including gold NPs, iron oxide NPs, semiconductor quantum dots (QDs), polymer NPs, carbon NPs, graphene, have been explored as the potential 55 candidates for integrating different functions<sup>[9][11]</sup>.

Carbon is generally recognized as a black material and till years ago, it was hard to accept that it could be soluble in water and even exhibit high fluorescence (FL)<sup>[11][12]</sup>. Nanoscience creates wonderful opportunities for scientific and technological expansions, such as synthesized nanosized carbon structures which possess completely different properties from the macroscopic material <sup>[13]</sup>.

Carbon quantum dots (CQDs) are a novel class of carbon nanomaterials with sizes below 10 nm, first found through purification of single-walled carbon nanotubes with preparative electrophoresis. CQDs have slowly become a valuable structure in the nanocarbon family.

## Introduction

---

There has been an increasing interest in Carbon Quantum Dots (CQDs) as a new class of carbon nanoparticles since its accidental discovery in 2004. This interest is attributed to following merits of CQDs<sup>[14][15]</sup>.

### Merits of CQDs

- Non-toxic
- Abundant
- Low-cost nature
- Strong Florescence (FL) and comparatively better solubility,
- Chemical inertness
- Easy modification and high resistance to photobleaching

Though the CQDs have enormous application in many fields such as biosensing, bioimaging, photocatalysis, optronics, solar cells, light emitting diodes. Their biomedical applications and targeting nature make it is more important in cancer studies.

Fluorescent carbon dots (CDs) with a size smaller than 10 nm, 60 excellent biocompatibility, low to none cytotoxicity, high quantum yield, non-blinking, and low cost, are considered as a rising star in nanomedicine.

However, in terms of emission tunability, the control over the emission of CDs is still in progress with increased understanding of the interplay between the surface states and intrinsic states in photoluminescence. Also, it has been reported that some food-based C-dots show anticancer properties, which strongly relies on the starting material employed for the synthesis. Fluorescent C-dots have been synthesized by a green one-pot hydrothermal route, using natural substances do not exhibit any significant toxicity to non-cancerous cells<sup>[15][16]</sup>,

## **Preparation methods**

During the last decade, several techniques have been suggested to prepare CQDs, which can be modified through synthesis or post-treatment.

## **Drawbacks facing CQDs preparation**

- (i) Agglomeration of CQDs, that could be evaded by applying electrochemical synthesis, and limited solution chemistry techniques,
- (ii) Uniformity and size control, which can be achieved through post-treatment processes such as centrifugation, dialysis and gel electrophoresis and
- (iii) Surface properties which are determinant factors for solubility and specific applications, which can be adjusted through synthesis or post-treatment

## **Electrochemical synthesis**

This technique is one of the most prominent top-down methods of producing CQDs using relatively large carbon materials including graphene, graphite, carbon fibre, etc. Advantages of electrochemical method are ease of operation, abundance of raw materials, potential for mass production, low cost and not involving any harsh or toxic chemicals <sup>[20][21]</sup>. However, tedious purification process of synthesized particles can be considered as a main disadvantage of this method

## **Chemical ablation**

This technique applies oxidizing acids to carbonize organic molecules, in which careful control over oxidation can lead to tinier CQDs. In this method, variety of accessible materials can be applied as precursor. However, the required

harsh circumstances and drastic procedures could be disadvantages of this method.

### **Supported synthesis technique**

Supported synthetic technique has been commonly used for the preparation of uniform and mono-disperse nanostructures, porous carbon and also CQDs. In the first step, satellite-like polymer/F127/silica composites were produced by an aqueous based technique employing silica colloid spheres functionalized with amphiphilic triblock copolymer F127 (EO106PO70EO106, Mw ¼12,600; EO ¼ ethylene oxide, PO ¼ propylene oxide) as carriers and resols (phenol/ formaldehyde resins, Mw as carbon starting material. Thereupon, the nanosized CQDs were obtained by high temperature treatment and removal of silica carriers. Furthermore, acid treatment and simple surface passivation generated water-soluble, multicolour photoluminescent CQDs, this wet-chemistry-based procedure was suggested to be a flexible economical technique for synthesis of photoluminescent CQDs.

### **Microwave/ultrasonic synthesis**

This technique has been a very significant procedure in synthetic chemistry and offers different advantages such as being non-toxic, facile, scalable and low-cost. However, poor control over size of obtained particles is one of its main disadvantages

### **Laser ablation**

Laser ablation is facile, eco-friendly and effective method which is applied for production of carbon-derived nanomaterials including CQDs in which the surface particles are tunable.

### **Size control**

## Introduction

---

Controlling the size of CQDs is a critical step to reach stable properties for specific applications. Up to now, numerous investigations have been done to attain uniform and homogeneous CQDs through synthesis or post-treatment. As reported in most of researches, the prepared CQDs particles were refined through dialysis, filtration, gel-electrophoresis, column chromatography and centrifugation. Also, uniform and tunable-size CQDs can be obtained employing limited pyrolysis of organic materials as precursor in nanoreactors. This method can be divided into three steps as follows (i) impregnating silica spheres as nanoreactors with carbon precursor through capillary force, (ii) pyrolysing the confined carbon precursor and (iii) eliminating nanoreactors to release the obtained CQDs. In this method, pore diameter of porous nanoreactors is the most important parameter that determines the size and size distribution of final CQDs. Porous silicas are common nanoreactors due to their thermal stability, tunability, availability of textures and easy removal [23][25].

### Surface modification

One of the most common techniques to change the surface properties of nanomaterials for particular applications is surface modification. In recent years, numerous investigations were performed for functionalizing and modifying the surface of CQDs including p-p interactions, sol-gel, coordination and covalent bonding. CQDs have high amount of oxygen-containing groups that let them to covalently bind with other functional groups. Covalent bonding with chemical agents containing amine groups is a current approach for surface modification to reclaim the PL of CQDs [13].

### PROPERTIES CQDs

#### a) Absorbance

CQDs usually have apparent optical absorption in the UV-visible region. Most of the CQDs, no matter how they are synthesized, possess an absorption band around 260–323 nm. In some cases, the n-p transition of C<sup>1</sup>/O bonds or the p-p transition of the C<sup>1</sup>/C bonds may cause absorption shoulders in absorption

spectra. It is found that surface passivation of CQDs with various molecules results in a shift of absorbance to longer wavelength.

**b) Photoluminescence**

The size-dependent optical absorption or PL is the classic sign of quantum confinement, which is one of the most exciting features of CQDs. The clear reliance of the emission wavelength and intensity on excitation is one the fascinating features of the PL of CQDs, whether it is because of various sizes of nanoparticles or diverse emissive traps that exist at the surface of CQDs.

**c) Electrochemical luminescence**

ECL is a parameter which is widely applied to explore the fluorescent emission of semiconductor nanocrystals such as QDs.

**d) Up-conversion photoluminescence (UCPL)**

Due to the many promising applications of up-conversion FL materials, especially in biomedical imaging, they have attracted much recent attention.

**e) Cytotoxicity**

Recently, wide range of investigations has been done in producing bio-probes based on bright CQDs with high stability. Although, the serious issue for applications of functionalized CQDs in live tissues, cells, and animals is their biocompatibility<sup>[26][28]</sup>.

### APPLICATIONS

**a) Bioimaging**

CQDs possess great potential for fluorescent bioimaging due to their superior fluorescent properties, possibility of multimodal bioimaging of cells and tissues, biocompatibility and low toxicity.

**b) Photocatalysis**

## Introduction

---

One of the important and also exiting fields in nanochemistry is nano-photocatalysis, in which designing a strong nanocatalyst with tunable chemical activity is considered as the main object.

### c) **Biosensor**

Due to good biocompatibility, excitation-dependent multicolour emission, high photostability, superior cell permeability, good water solubility and surface modification capability of CQDs, they are promising candidate as biosensor agents.

### d) **Drug delivery**

In recent years, nanotechnology-based drug delivery systems (DDSs) have been widely developed and various nanomaterials such as graphene oxides, polymeric nanoparticles, MS and Goldnanoparticles(AuNPs) have been investigated. as drug delivery vehicles. AuNPs were the most investigated nanoparticles as DDSs, but due to their toxicity and biocompatibility issues they encountered various limits in clinical applications <sup>[13]</sup>

This work attempts to synthesis COQ from natural vegetable source, by green synthesis extraction method from *Annona muricata* L. and screen its anticancer properties. Further, this study is attempted to conjugate anticancer drug sorafenib to the synthesised CQDs and evaluate its anticancer properties. So, the objective of this work is to synthesis low toxic natural based carbon Quantum Dots and its conjugate which can target only the cancerous cells<sup>[29][30]</sup>.

# Review of Literature

---

## REVIEW OF LITERATURE

1. **Pardo *et al.*, 2018**, reviewed on cancer Targeting and Drug Delivery Using Carbon-Based Quantum Dots and Nanotubes, Carbon-based nanoparticles have attracted attention in recent years due to their ability to act as a platform for the attachment of several drugs and/or ligands. Relatively simple models are often used in cancer research, wherein carbon nanoparticles are conjugated to a ligand that is specific to an over express recept or for imaging and drug delivery in cancer treatment.<sup>[6]</sup>
2. **Ding *et al.*, 2017**, investigated facile synthesis of red-emitting carbon dots from pulp-free lemon juice for bioimaging, in this work, red-emitting carbon dots with a high quantum yield of 28% in water were synthesized for the first time by heating an ethanol solution of pulp-free lemon juice. The obtained R-CDs were mono-dispersed with an average diameter of 4.6 nm, and exhibited excitation-independent emission at 631 nm. Meanwhile, these R-CDs featured low cytotoxicity and good photostability, which allow to be employed as luminescent probes for in vitro/in vivo bioimaging.<sup>[10]</sup>
3. **Zhenget *al.*, 2015**, investigated self-targeting fluorescent Carbon Dots for Diagnosis of BrainCancer Cells, A new type of carbon dots (CD-Asp) with targeting function toward brain cancer glioma was synthesized via a straightforward pyrolysis route by using D-glucose and L-aspartic acid as starting materials. The as-prepared CD-Asp exhibits not only excellent biocompatibility and tunable full-color emission, but also significant capability of targeting C6 glioma cells without the aid of any extra targeting molecules. In vivo fluorescence images showed high contrast biodistribution of CD-Asp 15 min after tail vein injection. Much stronger fluorescent signal was detected in the glioma site than that in normal brain, indicating their ability of freely penetrating blood-brain barrier and precisely targeting at glioma tissue.<sup>[2]</sup>

## Review of Literature

---

4. **Wang *et al.*, 2014**, reviewed on studied on synthesis, properties and applications of carbon quantum dots, which are generally small carbon nanoparticles (less than 10 nm in size) with various unique properties, have found wide use in more and more fields during the last few years. They have described the recent progress in the field of CQDs, focusing on their synthetic methods, size control, modification strategies, photoelectric properties, luminescent mechanism, and applications in biomedicine, optronics, catalysis and sensor issues. [3].
5. **Thakur *et al.*, 2014**, investigated antibiotic conjugated fluorescent carbon Dots as a Theranostic Agent for Controlled Drug Release, Bioimaging, and Enhanced Antimicrobial Activity. They have used microwave assisted synthesis of bright carbon dots using gum arabic and its use as molecular vehicle to ferry ciprofloxacin hydrochloride, a broad spectrum antibiotic. Density gradient centrifugation was used to separate different types of C-dots. After careful analysis of the fractions obtained after centrifugation, ciprofloxacin was attached to synthesize ciprofloxacin conjugated with C-dots.  
Release of ciprofloxacin was found to be extremely regulated under physiological conditions. [11].
6. **Modani *et al.*, 2013** have discussed about Quantum dots and its applications in medical field. They have pointed out that Quantum dots are considered as a new class of fluorescent labels which are robust and bright light emitters. Quantum dots are semiconductor nanocrystals ranging typically between 1-10 nanometers and have ability to glow or fluorescence brightly when excited by a light source such as a laser. They are composed of microscopic metal, thousand times smaller than width of a hair or semiconductor boxes such as cadmium selenide-zinc sulphide. They are considered as one of the highly innovative technology having wide applications in the field of biomolecular and cellular imaging [4].

## Review of Literature

---

7. **Ramezani *et al.*, 2018** have discussed about High stable and luminescent multicolor carbon quantum dots (CQDs) were prepared using quince fruit (*Cydonia oblonga*) powder as carbon precursors in one pot via microwave irradiation. Characterised by microscopic and 0.07 nm. The spectroscopic techniques. The results reveal that average size of the prepared particles was 4.85nm. CQDs have maximum emission intensity at 450 nm if excited at 350 nm with a quantum yield of 8.55%. CQDs prepared via microwave in 30 min were compared with those synthesized hydrothermally in a Teflon-lined stainless steel body autoclave at 200.<sup>[5]</sup>
8. **Iannazzo *et al.*, 2019** this study discussed the new generation members of graphene-family, have shown promising applications in anticancer therapy. In this study, they report the synthesis of a fluorescent and biocompatible nanovector, based on GQD, for the targeted delivery of an anticancer drug with benzofuran structure (BFG) and bearing the targeting ligand riboflavin (RF, vitamin B2). The highly water-dispersible nanoparticles, synthesized from multi-walled carbon nanotubes (MWCNT) by prolonged acidic treatment, were linked covalently to the drug by means of a cleavable PEG linker while the targeting ligand RF was conjugated to the GQD by  $\pi$ - $\pi$  interaction using a pyrene linker. The cytotoxic effect of the synthesized drug delivery system (DDS) GQD-PEG-BFG Pyr-RF was tested on three cancer cell lines and this effect was compared with that exerted by the same nanovector lacking the RF ligand (GQD-PEG-BFG) or the anticancer drug (GQDPyr-RF). The results of biological tests underlined the low cytotoxicity of the GQD sample and the cytotoxic activity of the DDS against the investigated cancer cell lines with a higher or similar potency to that exerted by the BFG alone, thus opening new possibilities for the use of this drug or other anticancer agents endowed of cytotoxicity and serious side effects<sup>[7]</sup>

## Review of Literature

---

9. **Weaver *et al.* 2009** this study discussed simple synthesis of quantum dot (QD)–polymer composites. Highly fluorescent semiconducting CdSe/ZnS quantum dots were embedded in different commercially available polymers using one easy step<sup>[9]</sup>.
10. **Deyet *al.*, 2011**, reviewed on Quantum Dot which can be used as novel carrier for drug delivery. They have expressed that quantum dots are nanoscale semiconductor crystals ranging typically between 1-10 nm and have capacity to glow or fluorescence brightly when excited by a light source such as a laser. Quantum dots are tiny bits of microscopic metal, thousand times smaller than width of a hair or semiconductor boxes such as cadmium selenide-zinc sulphide. Quantum dots are emerging as a new class of fluorescent probes for biomolecular and cellular imaging.
11. **Zenget *al.*, 2016**, investigated usage of carbon dots as a trackable drug delivery carrier for localized cancer therapy in vivo. In this report, for the first time they demonstrated that green-emitting CDs with carboxyl-rich surface can be employed as a trackable drug delivery agent 10 for localized cancer treatment in a mouse model. The CDs are conjugated with the cancer drug, Doxorubicin (DOX), via non-covalent bonding, utilizing the native carboxyl groups on CDs and the amine moiety on DOX molecule. The pH difference between cancer and normal cells was successfully exploited as the triggering mechanism for DOX release. They in vivo study demonstrated that the fluorescent CDs can serve as a targeted drug delivery system for localized therapy, and the stimuli 15 responsive non-covalent bonding between the nanodots carrier and the drug molecule is sufficiently stable in complex biological systems. <sup>[12]</sup>.
12. **Farshbafet *al.*, 2017** reviewed on carbon quantum dots and its recent progresses on synthesis, surface modification and applications. They have emphasized that carbon nanoparticles with a size of 10 nm (or less) are called carbon quantum dots (CQDs, C-dots or CD), which have created huge excitement due to their advantages in chemical inertness, high water

## Review of Literature

---

solubility, excellent biocompatibility, resistance to photobleaching and various optical superiority. They have described the recent advancements in the area of CQDs; concentrating on their synthesis techniques, size control, surface modification approaches, optical properties, luminescent mechanism, and their applications in bioimaging, biosensing, drug delivery and catalysis.<sup>[13]</sup>

13. **JafarMolaei et al., 2019** studied about carbon quantum dots and their biomedical and therapeutic applications. He emphasized that the fluorescence in CQDs originates from two sources, the fluorescence emission from bandgap transitions of conjugated p-domains and fluorescence from surface defects. The CQDs can emit fluorescence in the near-infrared (NIR) spectral region which makes them appropriate for biomedical applications. The fluorescence in these structures can be tuned with respect to the excitation wavelength. The CQDs have found applications in different areas such as biomedicine, photocatalysis, photosensors, solar energy conversion, light emitting diodes (LEDs), etc. The biomedical applications of CQDs include bioimaging, drug delivery, gene delivery, and cancer therapy. The fluorescent CQDs have low toxicity and other exceptional physicochemical properties in comparison to heavy metals semiconductor quantum dots (QDs) which make them superior candidates for biomedical applications. He clarified the synthesis routes and optical properties of the CQDs and recent advances in CQDs biomedical applications in bioimaging (in vivo and in vitro), drug delivery, cancer therapy, their potential to pass blood–brain barrier (BBB), and gene delivery.<sup>[30]</sup>
14. Joe Weaver *et al.*, **2009** investigated synthesis and characterization of quantum dot–polymer composites. They demonstrated a facile and simple synthesis of quantum dot (QD)–polymer composites. Highly fluorescent semiconducting CdSe/ZnS quantum dots were embedded in different commercially available polymers using one easy step. QD–polymer

## Review of Literature

---

composite nanoparticles were also synthesized using template-assisted synthesis. In particular, they self-assembled lamellar micelles inside nanoporous alumina membranes which were used for the synthesis of mesoporous silica hollow nanotubes and solid nanorods. They observed that the addition of excess free octadecylamine (ODA) in the QD–silica solution resulted in gelation. The gelation time was found to be dependent on free ODA concentration. Similarly, the emission of QD–polymer composites was also found to be dependent on free ODA concentration. Highly purified QDs provided polymer composites that have a much lower emission compared to unpurified nanocomposites. This was attributed to passivation of the QD surfaces by amine, which reduced the surface defects and non-radiative pathways for excited QDs. Finally, highly fluorescent QD–polymer patterns were demonstrated on glass substrates which retained their emission in both polar and non-polar solvents.<sup>[9]</sup>

15. **Pardo Jet al., 2018.** These carbon nanoparticles confer unique properties to the imaging or delivery vehicle due to their nontoxic nature and their high fluorescence qualities. Chief among the ongoing research within carbon-based nanoparticles emerge carbon dots (C-dots) and carbon nanotubes (CNTs). In this review, the fore mentioned carbon nanoparticles will be discussed in their use within doxorubicin and gemcitabine based drug delivery vehicles, as well as the ligand-mediated receptor specific targeted therapy.[14] .
16. **Madani SY et al., 2013**Conjugating nanoparticles with biomolecules like QD-herceptin conjugates or QD-aptamer (Apt)-DOX conjugates provides many opportunities for improving many of the current challenges in cancer diagnosis and therapy. This paper reviews combinatorial nanoparticles designed and formulated for cancer imaging and therapy, including inorganic nanoparticles (quantum dots, iron oxide particles, gold nanoparticles and silica and carbon nanoparticles), polymeric nanoparticles (PLGA, PLGA-PEG, PAMAM), liposomes and lipid nanoparticles.<sup>[15]</sup>

## Review of Literature

---

17. **Mukerjee A, et al., 2012** Carbon nanotubes (CNT) and quantum dots (QDs) are the two nanoparticles, which have received considerable interest in view of their application for diagnosis and treatment of cancer. The amphiphilic nature of CNTs allows them to penetrate the cell membrane and their large surface area (in the order of 2600 m<sup>2</sup>/g) allows drugs to be loaded into the tube and released once inside the cancer cell.<sup>[16]</sup>
18. **Zulfajri M, et al., 2019** Recently, synthesis, characterization, and application of carbon dots have received much attention. Natural products are the effectual carbon precursors to synthesize carbon dots with fascinating chemical and physical properties. The prepared carbon dots were characterized by UV light, transmission electron microscopy, Raman, Fourier transform infrared, UV-vis, and fluorescence spectroscopy.<sup>[17]</sup>
19. **Kong T, et al., 2018** Carbon dots (CDs) are one of the most promising carbon-based materials in bioimaging and drug/gene delivery applications. materials and methods: Carbon dots were synthesized by means of a hydrothermal approach with mixing citric acid and ethylene diamine.<sup>[18]</sup>
20. **Wu Fet al., 2019**, Photosensitizers are light-sensitive molecules that are highly hydrophobic, which poses a challenge to their use for photodynamic therapy. Hence, considerable efforts have been made to develop carriers for the delivery of PSs. Herein, we synthesized a new theranostic nanoagent (CQDsPtPor) through the electrostatic interaction between the tetraplatinated porphyrin complex (PtPor) and the negatively charged CQDs. The size and morphology of as-prepared CQDs and CQDsPtPor were characterized by a series of methods, such as XRD, TEM, XPS, and FTIR spectroscopy. The CQDsPtPor composite integrates the optical properties of CQDs and the anticancer function of porphyrin into a single unit. The spectral results suggested the effective resonance

## Review of Literature

---

energy transfer from CQDs to PtPor in the CQDsPtPor composite. Impressively, the CQDsPtPor composite showed the stronger PDT effect than that of organic molecular PtPor, suggesting that CQDsPtPor is advantageous over the conventional formulation, attributable to the enhanced efficiency of  $^1\text{O}_2$  production of PtPor by CQDs. Thus, this CQDs-based drug nanocarrier exhibited enhanced tumor-inhibition efficacy as well as low side effects in vitro, showing significant application potential in the cancer therapy.<sup>[19]</sup>

21. **Jiang X, et al., 2018** Carbon quantum dots (CQDs) have emerged as promising materials for optoelectronic applications on account of carbon's intrinsic merits of high stability, low cost, and environment-friendliness. However, the CQDs usually give broad emission with full width at half maximum exceeding 80 nm, which fundamentally limit their display applications. Here we demonstrate multicolored narrow bandwidth emission (full width at half maximum of 30 nm) from triangular CQDs with a quantum yield up to 54-72%. Detailed structural and optical characterizations together with theoretical calculations reveal that the molecular purity and crystalline perfection of the triangular CQDs are key to the high color-purity. Moreover, multicolored light-emitting diodes based on these CQDs display good stability, high color-purity, and high-performance with maximum luminance of 1882-4762 cd m<sup>-2</sup> and current efficiency of 1.22-5.11 cd A<sup>-1</sup>. This work will set the stage for developing next-generation high-performance CQDs-based light-emitting diodes.<sup>[20]</sup>
22. **Dager Aet al., 2019** quantum dots (CDs) were widely investigated because of their tunable fluorescence properties and low toxicity. However, so far there have been no reports on in vivo functional studies of hair and skin derived CDs. Here, hair derived CDs (HCDs) and skin derived CDs (SCDs) were produced by using human hair and pig skin as precursors. The quantum yields (QYs) of HCDs and SCDs were quite high, compared to citric acid derived CDs (CCDs). HCDs and SCDs possess optimal

## Review of Literature

---

photostability, hypotoxicity and biocompatibility in zebrafish, indicating that HCDs and SCDs possess the capacity of being used as fluorescence probes for in vivo biological imaging. The long-time observation for fluorescence alternation of CDs in zebrafish and the quenching assay of CDs by ATP, NADH and  $\text{Fe}^{3+}$  ions demonstrated that the decaying process of CDs in vivo might be induced by the synergistic effect of the metabolism process. All results indicated that large batches and high QYs of CDs can be acquired by employing natural and nontoxic hair and skin as precursors. To our knowledge, this is the first time to report SCDs, in vivo comparative studies of HCDs, SCDs and CCDs as bioprobes, and explore their mechanism of photostability in zebrafish.<sup>[21]</sup>

23. **Dias *Cet al.*, 2019.** The adjustment of the emitting wavelength of carbon dots (CDs) is usually realized by changing the raw materials, reaction temperature, or time. This paper reported the effective synthesis of multicolor photoluminescent CDs only by changing the solvent in a one-step solvothermal method, with 1,2,4,5-tetraaminobenzene as both the novel carbon source and nitrogen source. The emission wavelengths of the as-prepared CDs ranged from 527 to 605 nm, with quantum yields (QYs) reaching 10.0% to 47.6%, and it was successfully employed as fluorescence ink. The prepared red-emitting CDs (R-CDs,  $\lambda_{\text{em}} = 605$  nm) and yellow-emitting CDs (Y-CDs,  $\lambda_{\text{em}} = 543$  nm) were compared through multiple characterization methods, and their luminescence mechanism was studied. It was discovered that the large particle size, the existence of graphite Ns, and oxygen-containing functional groups are beneficial to the formation of long wavelength-emitting CDs. Y-CDs responded to crystal violet, and its fluorescence could be quenched. This phenomenon was thus employed to develop a detection method for crystal violet with a linear range from 0.1 to 11  $\mu\text{M}$  and a detection limit of 20 nM.<sup>[22]</sup>

## Review of Literature

---

24. **Zhang XDet *al.*, 2019** This study aims to obtain water-soluble fluorescent carbon dots (C-dots) from low-value metabolites through a simple, economical, one-step synthetic route. The urine C-dots (UCDs) and hydrothermally treated urine C-dots (HUCDs) were obtained, respectively, using straightforward Sephadex filtration method from human adults and hydrothermal reaction method. The UCDs and HUCDs emit fluorescence upon being excited with ultraviolet light with a quantum yield of 4.8% and 17.8%, respectively. TEM analysis revealed that UCDs and HUCDs had an average size of 2.5 nm and 5.5 nm, respectively. X-ray photoelectron spectroscopy (XPS) analysis showed the UCDs and HUCDs were mainly composed of carbon, oxygen and nitrogen. Fourier-transform infrared (FTIR) spectroscopy demonstrated the presence of functional groups, such as amino, hydroxyl, carboxylate and carbonyl groups onto the C-dots. The UCDs and HUCDs can be directly used for *in vivo* and *in vitro* imaging in HeLa cells, *Caenorhabditis elegans*, onion epidermal cells and bean sprouts. The cytotoxicity study revealed that the UCDs and HUCDs were not toxic to normal rat kidney (NKR) cells with good biocompatibility. The results revealed that the C-dots derived from urine have good biocompatibility, strong fluorescence and may have potential to be a safe fluorescent probe for bio-imaging.<sup>[23]</sup>
25. **Shi Y, *et al.*, 2019**The unique properties of carbon dots make it as an ideal carrier for incorporation of cancer targeting moieties, bio-imaging agents and antineoplastic agents in one delivery system. Results: Numerous applications of carbon dots in cancer theranostics have been reported during the past 10 years. This review introduces a brief history and basic fluorescent properties of carbon dots, and then discusses synthesis strategies and applications of carbon dots in biological imaging, targeted anti-cancer drug delivery, photodynamic therapy, photothermal therapy as well as gene delivery for cancer theranostics.<sup>[24]</sup>

## Review of Literature

---

26. **Bhatt Set al., 2018** Facile synthesis of carbon quantum dots with high fluorescence and excellent biocompatibility from plentiful and biocompatible materials still attracts much attention because of their great potential value in sensors and imaging. In this study, a highly fluorescent and super biocompatible N-doped carbon quantum dots derived from green precursor of aminated alkali lignin has been synthesized for cellular imaging.<sup>[25]</sup>
27. **Dong Y, et al., 2015** We report a one pot green strategy for the synthesis of carbon dots using tulsi leaves and their potential application in sensing of Cr(VI) selectively. Also the low toxicity, high fluorescence and photostability of the CDs make them excellent imaging and patterning agent. The acid and alkali resistant property of these CDs makes it suitable for real sample analysis.<sup>[26]</sup>
28. **Kanget al., 2015** Further, their potentials have also been verified in multifunctional diagnostic platforms, cellular and bacterial bio-imaging, development of theranostics nanomedicine, etc. This review provides a concise insight into the progress and evolution in the field of CQD research with respect to methods/materials available in bio-imaging, theranostics, cancer/gene therapy, diagnostics, etc.<sup>[29]</sup>
29. **Song J, et al., 2019** Carbon dots (CDs) have shown great promise in a wide range of bioapplications due to their tunable optical properties and noncytotoxicity. For the first time, a rational strategy was designed to construct new bio-nanoplatfroms based on carboxylic acid terminated CDs (CDs-COOH) conjugating with amino terminated F-substituted nano-hydroxyapatite (NFAP) via EDC/NHS coupling chemistry. The monodisperse NFAP nanorods were functionalized with o-phosphoethanolamine (PEA) to provide them with amino groups and render them hydrophilic with respect to the ligand exchange process. The CDs-COOHPEA-NFAP conjugates exhibits bright blue fluorescence under UV illumination, excellent photostability and colloidal stability. Due to

## Review of Literature

---

their low cytotoxicity and good biocompatibility as determined by methyl thiazolyl tetrazolium (MTT) assay, the CDs-COOHPEA-NFAP conjugates were successfully applied as bio-nanoplatfoms to MCF-7 breast cancer cells for cellular imaging *in vitro*. More importantly, the functional CDs conjugated to NFAP provide an extended and general approach to construct different water-soluble NFAP bio-nanoplatfoms for other easily functionalised luminescent materials. Therefore, these green nanoplatfoms may be a prospective candidate for applications in bioimaging or targeted biological therapy and drug delivery.<sup>[27]</sup>

30. **Zhao Y, et al., 2014** This paper reports turn-off fluorescence sensor for Fe (3+) ion in water using fluorescent N-doped carbon dots as a probe. A simple and efficient hydrothermal carbonization of *Prunus avium* fruit extract for the synthesis of fluorescent nitrogen-doped carbon dots (N-CDs) is described. The green synthesized N-CDs are efficiently used as a promising candidate for the detection of Fe (3+) ions and bio-imaging.<sup>[28]</sup>
31. **Radyet al., 2018** This study shows Graviola (*Annona muricata*) is a small deciduous tropical evergreen fruit tree, belonging to the Annonaceae family, and is widely grown and distributed in tropical and subtropical regions around the world. The aerial parts of graviola have several functions: the fruits have been widely used as food confectionaries, while several preparations, especially decoctions of the bark, fruits, leaves, pericarp, seeds, and roots, have been extensively used in traditional medicine to treat multiple ailments including cancers by local communities in tropical Africa and South America. The reported therapeutic benefits of graviola against various human tumors and disease agents in *in-vitro* culture and preclinical animal model systems are typically tested for their ability to specifically target the disease, while exerting little or no effect on normal cell viability. Over 212 phytochemical ingredients have been reported in graviola extracts prepared from different plant parts. The specific bioactive constituents responsible for the major anticancer,

## Review of Literature

---

antioxidant, anti-inflammatory, antimicrobial, and other health benefits of graviola include different classes of annonaceous acetogenins (metabolites and products of the polyketide pathway), alkaloids, flavonoids, sterols, and others. This review summarizes the current understanding of the anticancer effects of *A. muricata* and its constituents on diverse cancer types and disease states, as well as efficacy and safety concerns. It also includes discussion of our current understanding of possible mechanisms of action, with the hope of further stimulating the development of improved and affordable therapies for a variety of ailments.<sup>[31]</sup>

32. **Zhao *et al.*, 2017** investigated use of Urethane acrylate (UA) was used to prepare carbon quantum dots (C-dots) luminescent membranes. It was examined by FT-IR, mechanical strength, scanning electron microscope (SEM) and quantum yields (QYs)<sup>[32]</sup>
33. **Zhang, *et al.*, 2018** reviewed on preparing natural-product-derived carbon dots (NCDs), because natural products have several advantages. First, natural products are renewable and have good biocompatibility. Second, natural products contain heteroatoms, which facilitate the fabrication of heteroatom-doped NCDs without the addition of an external heteroatom source. Finally, some natural products can be used to prepare NCDs in ways that are very green and simple relative to traditional methods for the preparation of carbon dots from man-made carbon sources. NCDs have shown tremendous potential in many fields, including biosensing, bioimaging, optoelectronics, and photocatalysis.<sup>[6]</sup>
34. **Li K, *et al.*, 2018**, reviewed on Fluorescent graphene quantum dots (GQDs) have attracted increasing interest in cancer bioimaging due to their stable photoluminescence (PL), high stability, low cytotoxicity, and good biocompatibility. The recent applications study shows GQDs in cancer bioimaging are demonstrated in detail, in which we focus on the biofunctionalization of GQDs for specific cancer cell imaging and real-time molecular imaging in live cells<sup>[33]</sup>

## Review of Literature

---

35. **Vasimalaet *al.*, 2018** developed aqueous fluorescent C-dots have from cinnamon, red chilli, turmeric and black pepper, by a one-pot green hydrothermal method. The synthesized C-dots were firstly characterized by means of UV-vis, fluorescence, Fourier transform infrared and Raman spectroscopy, dynamic light scattering and transmission electron microscopy. The optical performance showed an outstanding ability for imaging purposes, with quantum yields up to 43.6%. Thus, the cytotoxicity of the above mentioned spice-derived C-dots was evaluated in vitro in human glioblastoma cells (LN229 cancer cell line) and in human kidney cells (HK-2 non-cancerous cell line). Bioimaging and viability studies were performed with different C-dot concentrations from 0.1 to 2  $\text{mg}\cdot\text{mL}^{-1}$ [1]

## **Aim and objectives**

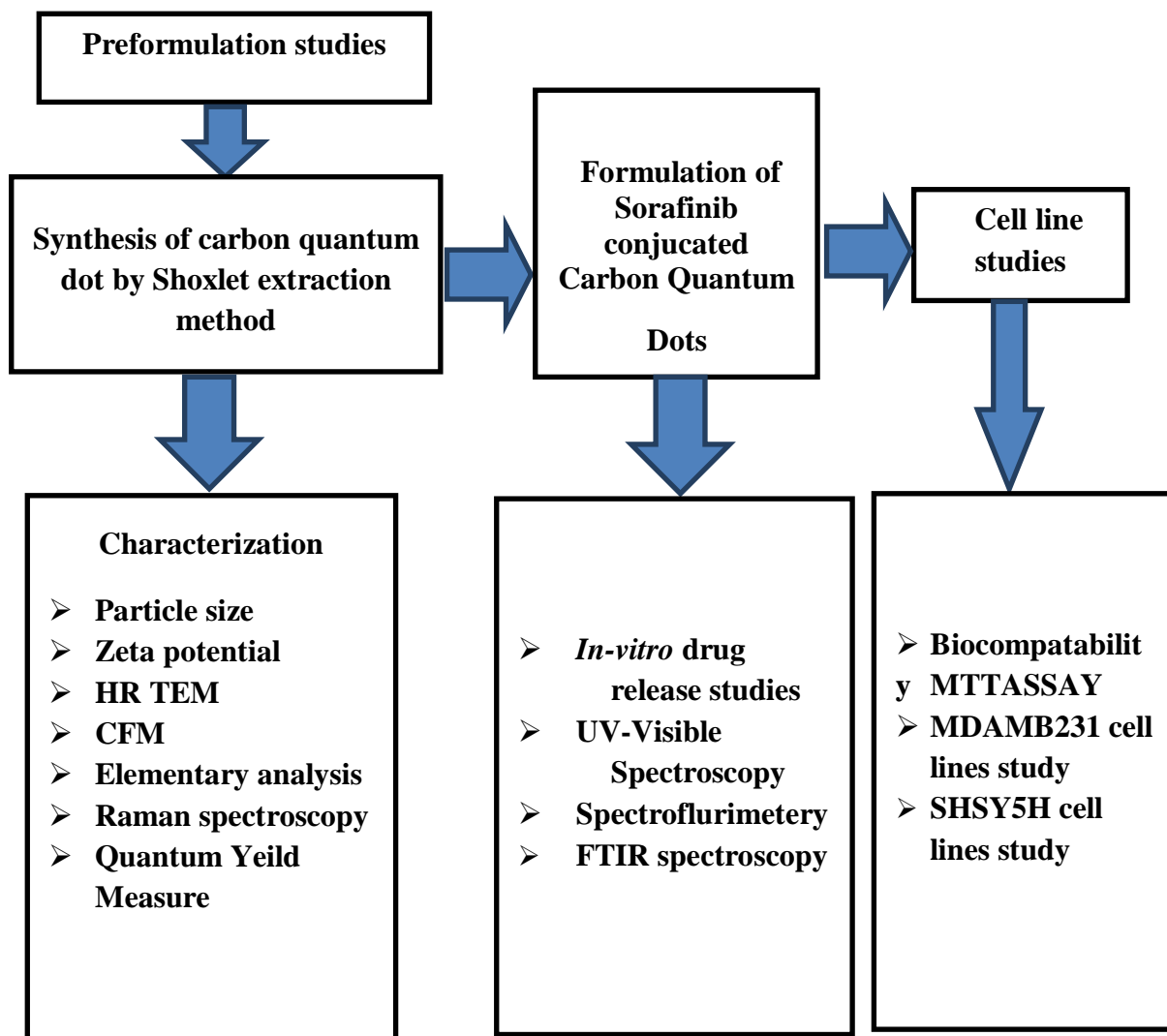
---

### **AIMS AND OBJECTIVES**

This study is planned to fulfill the following aims and objectives

- To synthesis low cost carbon based targeted drug delivery system from a natural precursor for cancer treatment.
- To develop low dose and high therapeutic action Sorafinib conjugated Carbon Quantum Dots.
- To reduce the side effect of Sorfinib by developing it as Carbon Quantum Dot .
- To formulate and characterize carbon quantum dot by a novel extraction method.
- To evaluate the anticancer activity of synthesised carbon quantum Dots.
- To perform cyto toxicity study of Carbon Quantum Dots and conjugated Carbon Quantum Dots.

PLAN OF WORK



## Materials & Equipments

---

### MATERIALS AND EQUIPMENTS

#### MATERIALS USED

Sl. No	Materials	Source
1.	Sorafenib	Gift sample
2.	Sodium tripolyphosphate	Sigma Aldrich
3.	<i>Annona muratica</i> L.	Natural source
4.	Ethanol	Zhuhai Chemico Industries
5.	Di-Sodium Hydrogen Orthophosphate	SD Fine Chemical Limited
6.	Potassium Dihydrogen Orthophosphate	Qualigens Fine Chemicals, Mumbai

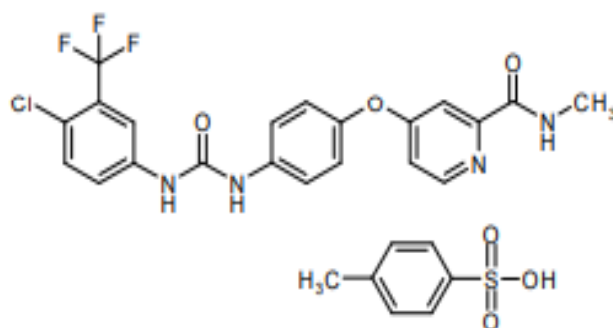
#### EQUIPMENTS USED

Sl. No	Equipment	Model/ Company
1.	Magnetic stirrer	REMI-2MLH
2.	Spectrofluorimetry	MOTIC B1 SERIES
3.	UV Spectrophotometer	JASCO V-530
4.	FT-IR Spectrometer	FTIR JASCO -4100
5.	Ramanspectroscopy	WiTec alpha 300, Germany
6.	Zeta Sizer	Malvarin zeta sizer (USA)
7.	HR TEM	(The JEOL JEM 2100)
8.	Elementary analysis	(The JEOL JEM 2100)
9.	Confocal microscope imaging	Nikon H6001 made in japan

### DRUG PROFILE

- Proper name** : Sorafenibtosylate
- Chemical name** : 4-(4-(3-[4-Chloro-3-(trifluoromethyl)phenyl]-ureido)phenoxy)- N methylpyridine-2-carboxamide  
4-methylbenzenesulfonatey
- Molecular formula** :  $\text{C}_{21}\text{H}_{16}\text{ClF}_3\text{N}_4\text{O}_3 \times \text{C}_7\text{H}_8\text{O}_3\text{S}$
- Molecular weight** : 637.0 g/mole

**Structural formula:**



- Melting point** : 205.6 °C
- Boiling point** : 523.3±50.0 °C at 760 mmHg
- Density** : 1.5±0.1 g/cm<sup>3</sup>
- Colour** : Sorafenib is white to Yellowish or brown
- Solubility** : Slightly soluble in ethanol and soluble in Polyethylene Glycol (PEG)400
- Storage** : 15°C–30°C

### **Mechanism of Action**

Sorafenib was shown to inhibit multiple intracellular (c-CRAF, BRAF and mutant BRAF) and cell surface kinases (KIT, FLT-3, RET, RET-PTC, VEGFR-1, VEGFR-2, VEGFR-3, and PDGFR- $\beta$ ). Several of these kinases are thought to be involved in tumour cell signaling, angiogenesis, and apoptosis.

Sorafenib inhibited cell proliferation of the human hepatocellular carcinoma PLC/PRF/5 and HepG2 cell lines, renal cell carcinoma (786-O cell line), differentiated thyroid carcinoma (TPC-1 cell line, carrying a RET/PTC1 rearrangement) and tumour growth of several human tumour xenografts (PLC/PRF/5 cell line) in immunocompromised mice. A reduction in tumour angiogenesis and increases in tumour apoptosis was seen in the xenograft models of human hepatocellular and renal cell carcinoma cell lines. Additionally, a reduction in Raf/MEK/ERK signaling was seen in human hepatocellular carcinoma PLC/PRF/5 and HepG2 cell lines, and the differentiated thyroid carcinoma TPC-1 cell line. A reduction of RET/PTC (a rearrangement commonly found in DTC) receptor autophosphorylation was observed in NIH/3T3 cells transfected with RET/PTC3.

### **Adverse Reactions:**

Diarrhea, Anorexia, Nausea, Vomiting, Constipation, Hypertension, Hemorrhage/bleeding, Cardiac ischemia/infarction, Renal failure, Dyspnea, Cough, Pleural effusion, Voice changes

### **Dosage and administration:**

Daily dose of NEXAVAR (sorafenib tablets) is 400 mg taken twice a day without food or with a low-fat or moderate.

For oral use.

### **Absorption:**

Administration of sorafenib tablets, the mean relative bioavailability is 38%-49% when compared to an oral solution.

### **Metabolism:**

Sorafenib is metabolized primarily in the liver undergoing oxidative metabolism mediated by CYP3A4 as well as glucuronidation mediated by UGT1A9

### **Elimination:**

77% of the dose excreted in feces, 19% of the dose excreted in urine, The elimination half-life of sorafenib is approximately 25-48 hours.

### **Indications**

Treatment of patients with unresectable hepatocellular carcinoma (HCC).

Treatment of locally advanced / metastatic Renal Cell (clear cell) Carcinoma (RCC) in patients who failed or are intolerant to prior systemic therapy.

Treatment of patients with locally advanced or metastatic, progressive differentiated thyroid carcinoma (DTC) refractory to radioactive iodine.

### **Contraindications:**

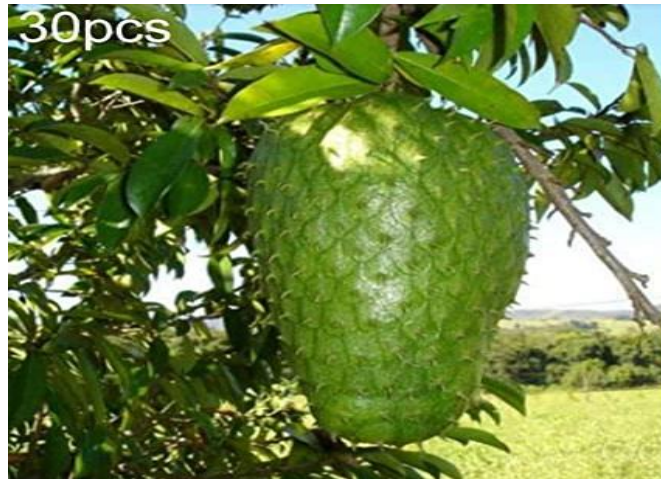
Hypertension, Hemorrhage, Cardiac ischemia/infarction, Gastrointestinal perforation, Drug-induced hepatitis,

### **Storage and Handling:**

Stored at controlled room temperature (15°C–30°C) in a dry place.

**Brand names** : NEXAVAR,

## PLANT PROFILE



**Synonym:** graviola, guyabano, guanábana, Annonamacrocarpa

**Botanical Name :** *Annonamuricata*L.

**Family :** Annonaceae

**Kingdom :** Plantae

**Genus :** Annona

**Species :** A. muricata

### **Description:**

*Annonamuricata*L is a small, upright, evergreen tree that can grow to about 30 feet (9.1 m) tall. The fruits are dark green and prickly. They are ovoid and can be up to 30 centimeters (12 in) long<sup>[9]</sup> with a moderately firm texture. Their flesh is juicy, whitish and aromatic.

### **Nutrition:**

Raw source contains 81% water, 17% carbohydrates, 1% protein

### **Phytochemicals:**

## Plant Profile

---

Compound annonacin is contained in the fruit, seeds, and leaves of the plant. The leaves of *Annonamuricata* L contain annonamine.

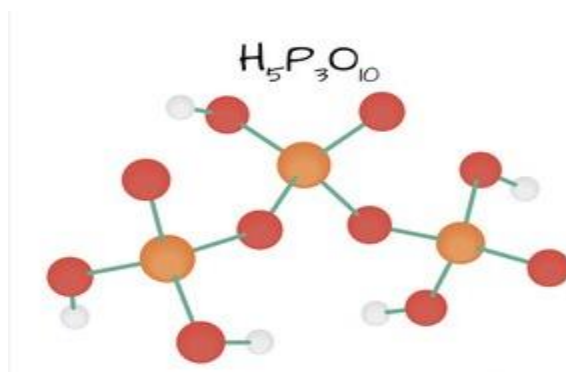
### Uses:

The flesh of the fruit consists of an edible, white pulp, some fiber, and a core of indigestible black seeds. The pulp is also used to make fruit nectar. Smoothness, fruit juice drinks, as well as candies, sorbets, and ice cream flavorings. (Radyet *al.*, 2018)<sup>[31]</sup>

### LINKER PROFILE

#### Sodium tripolyphosphate

##### Structure:



**Synonym** : Sodium triphosphate, Sodium tripolyphosphate, tripolyphosphate

**Molecular Formula** :  $\text{Na}_5\text{O}_{10}\text{P}_3 \cdot n\text{H}_2\text{O}$  (n = 0 or 6)

**Molecular Weight** : 367.86 g/mol

**Physical Description:** white crystals of powder

**Melting Point** : 22 °C

**Density** : 2.52 g/cm<sup>3</sup>

**pH:** Between 9,1 and 10,2 (1 % solution)

**Solubility** : Freely soluble in water, Insoluble inEthanol

##### USEs:

General adhesives and binding agents for a variety of trip. It binds strongly to metal cations as both a bidentate chelating agent and tridentate.

# Experimental Methods

---

## PREFORMULATION STUDIES

### Physical characteristics:

By visual examination the drug was tested for its physical characters like colour, odour and texture.

### Solubility test:

Sorafenib powder (about 1mg) was taken in a test tube and solubility in ethanol, water, dichloromethane and chloroform was tested.

### Construction of calibration curve of sorafenib:

#### 1) Preparation of stock solution:

The standard stock solution of sorafenib was prepared by transferring accurately weighed quantity (10 mg) of sorafenib raw material in 100 ml of volumetric flask. The drug was dissolved with the addition of few drops of Polyethylene glycol(1%), the volume was made up to 100 ml with ethanol to get a stock solution of 100 µg/mL Selection of Wavelength The standard stock solution was scanned in the range of 200 to 400 nm in UV spectrophotometer using phosphate buffer pH 6.8 as blank. The absorption maximum was found at 265 nm.

#### 2) Preparation of working stock solution

From the standard stock solution of sorafenib 0.5, 1, 1.5, 2, 2.5, 3, 3.5 and 4 ml were withdrawn to 10 ml volumetric flask and then made up volume with phosphate buffer pH 6.8 to get a concentration range of 5-40 µg/mL. The absorbance of these solutions was measured at 265nm using JASCO V-530 UV 1600 UV- visible spectrophotometer. Phosphate buffer pH 6.8 was used as blank. The calibration curve was plotted between concentration and absorbance.

### Synthesis of CQDs

## Experimental Methods

---

*Annona muricata* L. was obtained from a garden in thrissur district, Kerala, was authenticated by botanical survey of India, Tamil Nadu Agriculture University Coimbatore. The whole fruit *Annona muricata* L. powder was dried at about 60°C for 48 h. Then it was powdered and passed through a 60 mesh stainless steel sieve. Then the fruit powder was extracted using ethanol in Soxhlet extraction apparatus at 60°C for 72 h. Once the reaction was complete, the reactant was cooled to room temperature, a dark brown product was obtained, implying the formation of *Annona muricata* L. *annonamuricata*-derived CQDs. The resulting mixture was filtered by a piece of micro porous membrane with pore size of 0.45 µm to remove large particles. Vacuum evaporation at 40°C was carried out to obtain the residue. From the residue, CQDs were obtained by vacuum freeze-drying and stored in a well closed container and kept at 4°C for further studies [28]

### Quantum Yield Calculation

The quantum yield (QY) of the as-prepared CQDs was obtained according to an established spectrofluorometric method. Quinine sulfate was dissolved in 0.1 M H<sub>2</sub>SO<sub>4</sub> (F = 54%) as a standard. Both the absorbance of CQDs and quinine sulfate solutions were adjusted to below 0.1 to minimize inner filter. The QY of CQDs was determined by the following Equation:

$$QY_x = QY_{st} \left( \frac{I_x}{I_{st}} \right) \left( \frac{A_{st}}{A_x} \right) \left( \frac{n_x}{n_{st}} \right)^2$$

where I and A are the fluorescence integral intensity and absorbance, respectively. The refractive index (n), The subscripts x and st correspond to CQDs and quinine sulfate. [15]

### CHARACTERIZATION CQD

## Experimental Methods

---

### Zeta potential and particle size characterization

The size and morphology of CQDs were investigated using a Malvern zeta sizer (MAL1063652 Zetasizer Ver. 7.13) operated at an accelerating voltage of 200 kV (Mukerjee A, et al 2012)<sup>[16]</sup> and High resolution transmission electron microscopy (The JEOL JEM 2100) operated at 200 kV respectively<sup>[14]</sup>. The crystalline phase was investigated by a Malvern analytical multipurpose diffractometer.

### Raman effect

The Raman spectrum of as prepared CQD was recorded at ambient temperature in a Fluorescence microscopy images were captured using Confocal Raman Microscope with AFM imaging (WiTec alpha 300, Germany) fluorescence microscope at excitation wavelength of 50 nm - 400 nm<sup>[17]</sup>.

### Fourier transform infrared spectroscopy

The Fourier transform infrared (FTIR) spectra of synthesized CQD were measured by a Thermo shimadzu FTIR spectrometer with the KBr pellet technique ranging from 400 to 4000 cm<sup>-1</sup><sup>[18]</sup>.

### Spectrofluorimetry

Fluorescence spectroscopy of CQD was performed with a Horiba Fluoromax4 spectrophotometer at different excitation wavelength ranging from 310 to 480 nm. UV absorption spectra were obtained using a Shimadzu probe 2.0 UV spectrophotometer<sup>[5]</sup>.

### Confocal microscopic imaging

CQD imaging was done under confocal microscope with laser excitations of 405 and 488 nm. Finally, the imaging process is done under confocal microscope.<sup>[25]</sup>

### Preparation of sorafenib COQ-Dot Conjugates.

## Experimental Methods

---

For the synthesis of the sorafenib COQ-Dot conjugate, 0.5 mL (1000  $\mu$ M) sorafenib solution was added to 9.5 mL (95 mg/mL) C-dots with tripoly phosphoric acid (10%) and stirred for 3 h at 30°C. The change in the optical properties of sorafenib C-dots conjugate was studied using UV-Vis Spectroscopy in the spectra window of 200–800 nm with respect to pure C-dots.<sup>[19]</sup>

### Drug loading Efficiency

The entrapment efficiency of sorafenib COQ-Dot conjugate were determined by adding 10 ml of pH 6.8 phosphate buffer and sonicated in a bath sonicator and filtered. 1 ml of filtrate is made up to 10 ml with phosphate buffer and was assayed spectrophotometrically at 265 nm (UV visible spectrophotometer, model UV-1601 PC, Shimadzu). The amount of entrapped drug was calculated from the equation.

$$\text{Entrapment Efficiency(\%)} = \frac{(\text{Mean CQD absorbance} + \text{Pure sorafenib absorbance})}{\text{conjugate cqd absorbance}} \times 100$$

### Drug sorafenib COQ-Dot Conjugates Compatibility Studies:

FTIR spectrum of sorafenib, Tripoly phosphoric acid and conjugated COQ Dots were recorded using FTIR Spectro photometer (Shimadzu JASCO 4100). The diffuse reflectance technique was utilised in the mid IR 4000-400  $\text{cm}^{-1}$  spectral region. The procedure consists of dispersing the sample in KBr (100mg) using a mortar, triturating the materials into a fine powder bed into the holder using compression gauge. The pressure was around 5 tons for 5 minutes. The pellet was placed in the light path and the spectrum was recorded. The characteristic peaks of the functional groups were interpreted.<sup>[8]</sup>

### Diffusion study

The diffusion study of sorafenib COQ-Dot conjugate, was performed by

## Experimental Methods

---

diffusion cell method, diffusion cell having an area of 1.5cm, using specified (Phosphate buffer pH 6.8) as the receptor media. A small quantity of SNB-tablets (equivalent to 50mg of sorafinib COQ-Dot conjugate,) was placed on the egg yolk membrane surface, and after a specific time interval, sampling was performed (6, 12, 24, 30, 60, 120min) by removing the media from receptor compartment and replacing it with fresh medium. The collected sample was filtered and diluted, further analyzed using JASCO V-530 UV 1600 UV- visible spectrophotometer. The mean cumulative amount of drug release at each time point was calculated. [22]

### Cytotoxicity Studies.

Cytotoxic effect of the sorafinib COQ-Dot conjugate was studied on most commonly used using 3-(4,5-dimethyl-2-thiazolyl)-2,5-diphenyltetrazolium bromide (MTT) assay. SHSY5H and MDAMB231 cells were used for this study. Cells were plated into a 96 well plate at density of  $6 \times 10^3$  cells / well. The plate was incubated overnight in Co2 incubator for cell adherence. After incubation given test articles are added and incubated for 48 hrs. After 48 hrs of drug treatment, 10 $\mu$ L of MTT (5mg/ ml) reagent was added in each well and incubated. After 4 hr of incubation, the formazan crystal formation was observed under the microscope. Then, medium was removed and 100  $\mu$ L of DMSO was added for solubilizing the formazan crystals and kept 30 minutes at dark. The absorbance was measured using microplate reader at 560 nm<sup>[26]</sup>. Percentage viability was calculated using the formula,

$$\text{Percentage viability} = \frac{[(\text{absorbance of test} - \text{absorbance of blank})]}{[(\text{absorbance of control} - \text{absorbance of blank})]} \times 100$$

### RESULTS AND DISCUSSION

#### SYNTHESIS OF CQDs

CQOs were prepared by extraction method. The fruit AM contains branched cyclopeptides, polysaccharide, minerals. Due to the very high content of branched carbon and proteins, it could act as versatile raw material for the synthesis of highly fluorescent C-dots by extraction method. Color of AM (milk white) got transformed to wine red after heating for 15 min under the influence of Ethanol.

#### CHARACTERIZATION

##### Photoluminescence

Photoluminescence (PL) is due to surface energy traps and the quantum effect<sup>[5]</sup>. The quantum effect is related to particle size and causes blue emission. CQDs surface functional groups introduce different energy levels and consequently a red shift in emission. PL characteristics of the prepared CQDs prepared by method showed excitation-dependent PL (Fig. 1). It was reported that excitation-dependent emission is due to different energy levels incorporated into the CQDs by different surface groups such as C-O, C=O, O=C-OH. Passivation of the CQDs reduced the energy levels, and mono-color particles were produced. In fig 2 main absorption band is at 345 nm, which respectively correspond to aromatic ring's  $\pi \rightarrow \pi^*$  transitions<sup>[34, 35]</sup>. Under the normal light conditions, the CDs solution in water had a yellow-pale orange color as shown in Fig 2. The CDs emitted blue light under UV light. The fluorescence peak of CQDs 517nm appear

## Results & Discussion

---

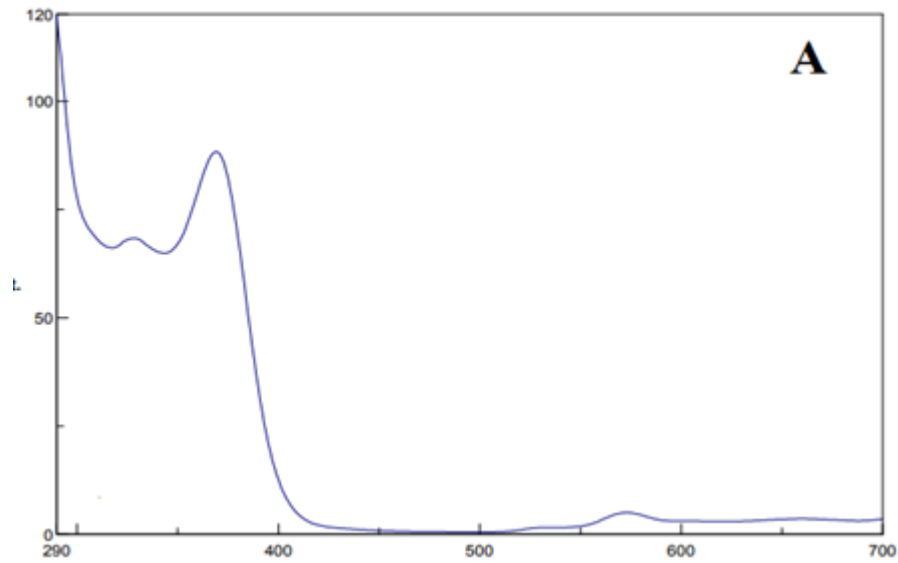
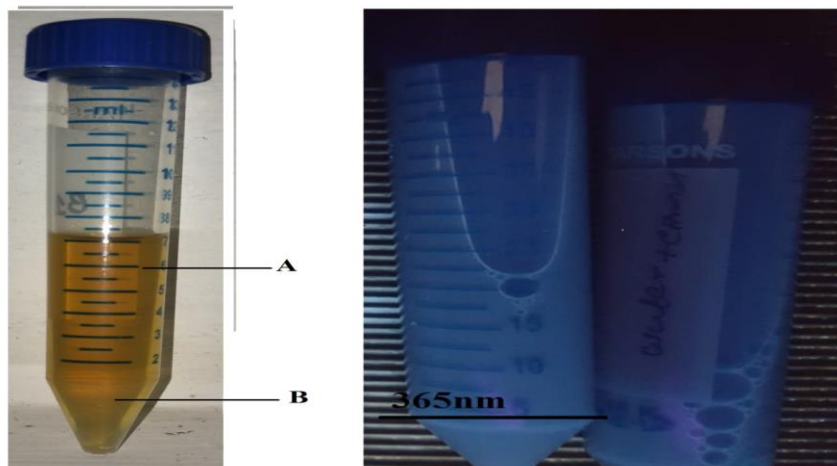


FIG 1: Emission spectrum of carbon dot



**Fig 2 The CQDs deposited on invert fluorescence in uv chamber and scanned between 365-700nm.**

### Stability of CQDs

CQDs were stable for more than two months while stored at 4 °C with less than 5% loss in intensity.

## Results & Discussion

### Quantum Yield Calculation

The quantum yield ( $\Phi$ ) of the CQDs was calculated using quinine sulfate as reference. Their fluorescence spectra were recorded at same excitation of 365 nm are shown Fig 2. By comparing the integrated photoluminescence intensities (excited at 365 nm) and the absorbency values (at 365 nm) of the carbon sample with the references quinine sulfate, quantum yield of the carbon sample was determined. The data was plotted and the slopes of the sample and the standards were determined. The data showed good linearity with intercepts of approximately zero and are shown in Fig 3. The quantum yield for CQDs found to be 25.6 % respectively.

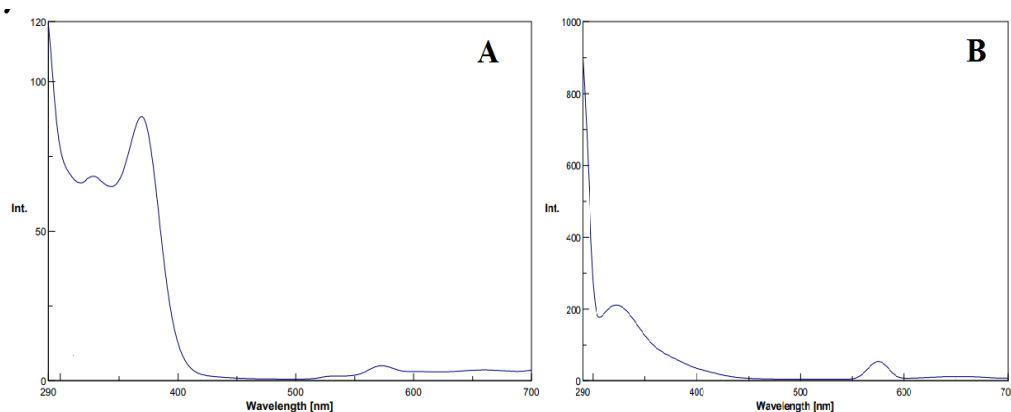


**Fig 3. Emission spectrum (a) quinine sulphate (b) carbon dots**

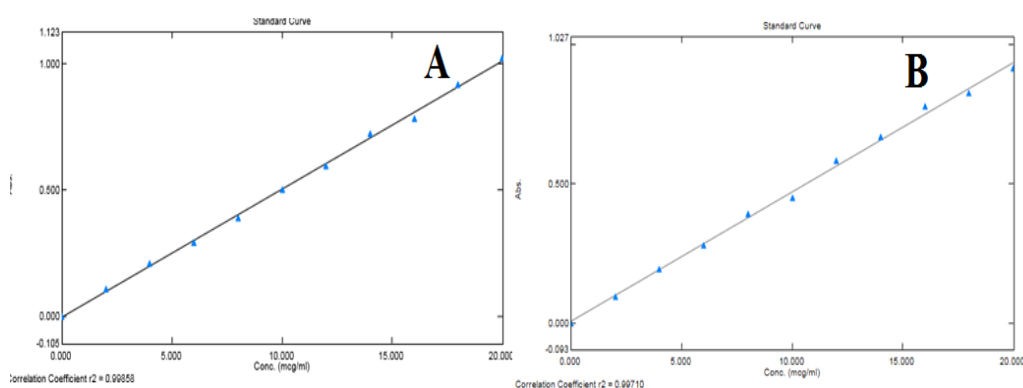


**Fig 4. Calibration plot of (A) Quinine Sulphate (B) CQDs**

## Results & Discussion

---

**Table: 1** Average Quantum yields of CQDs

CONCENTRATION(mcg/ml)	ABSORBANCE AT365nmQuinine Sulphate	ABSORBANCE AT(365nm)CQDS	QUANTUM YIELDAVERAGE(%)
2	0.107	0.096	25.6%
4	0.210	0.195	
6	0.291	0.177	
8	0.389	0.191	
10	0.500	0.249	
12	0.595	0.282	
14	0.723	0.269	
16	0.784	0.376	
18	0.914	0.327	
20	1.021	0.313	

### Particle Size Measurement

The particle size is one of the most important parameter for the characterization of CQDs. The average particle size of the formulated CQDs were measured using Malvern zeta sizer. Particle size analysis showed that the average particle size of CQDs was found to be  $27.53 \pm 9.45$  nm with polydispersity index (PDI) value 0.233 and with intercept 0.615. The average size of the CQDs is comparatively less than as that of the size works reported in many studies Ref

## Results & Discussion

	Size (d.nm):	% intensity:	St Dev (d.n...)
<b>Z-Average (d.nm):</b> 27.53	<b>Peak 1:</b> 37.11	100.0	20.76
<b>Pdl:</b> 0.233	<b>Peak 2:</b> 0.000	0.0	0.000
<b>Intercept:</b> 0.615	<b>Peak 3:</b> 0.000	0.0	0.000
<b>Result quality:</b> Good			

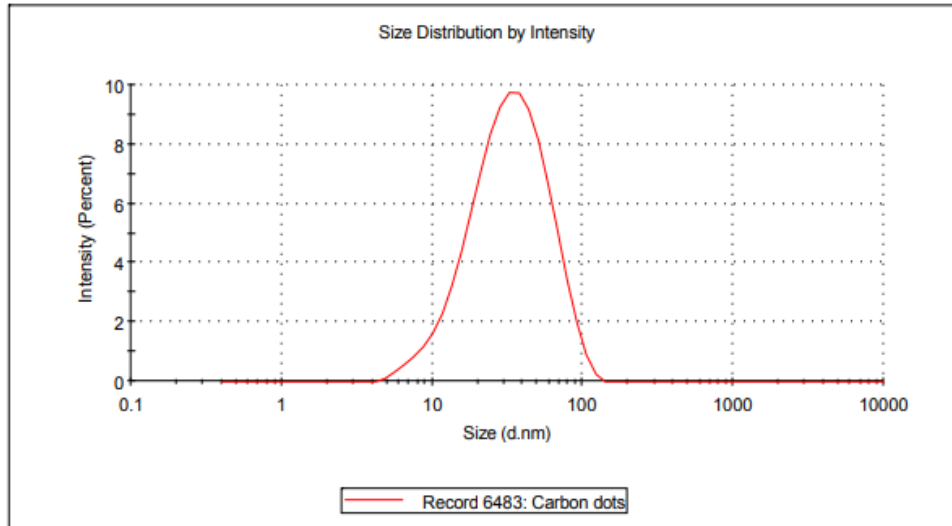


**Fig 5: Particle size distribution of CQDs Zeta potential determination of the CQDs**

The zeta potential of synthesized CQDs was recorded by Malvern Zeta Sizer. Data in Fig 5 identified that the particles are negatively charged with a zeta potential of -15.2. with peak area of 100% intensity. Having considered FTIR results, this negative charge is due to carboxylic groups on the surface. High zeta potential confirms a high degree of carboxylic functional

## Results & Discussion

groups.

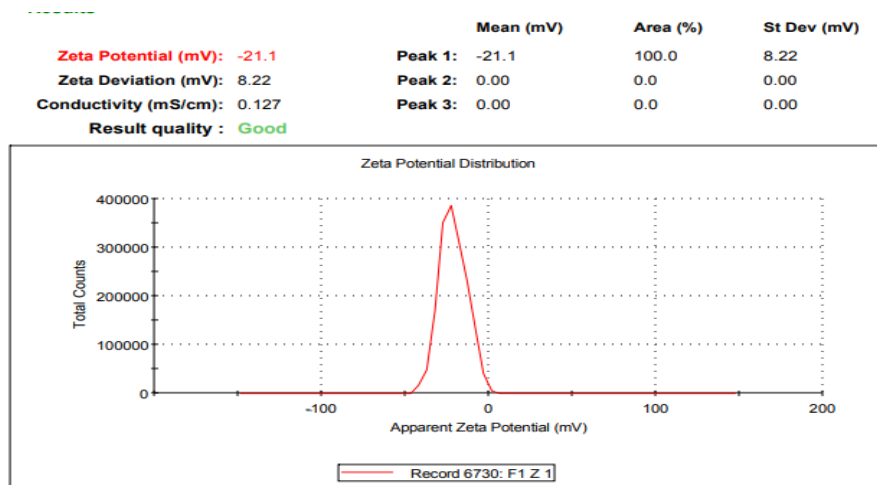


**Fig 6: Particle size distribution of CQDs High Resolution Transmission Electron Microscopy (HRTEM)**

HRTEM analyses were performed to evaluate the surface morphology of CQDs and conjugated carbon dot (SRN@cqdS). HRTEM images are shown in Fig 7. HRTEM images showed that CQDs have smooth surface morphology with porous in nature and are spherical in shape, the SRN@cqdS found to be smooth porous where outer surface was shiny smooth and inner surface was porous.

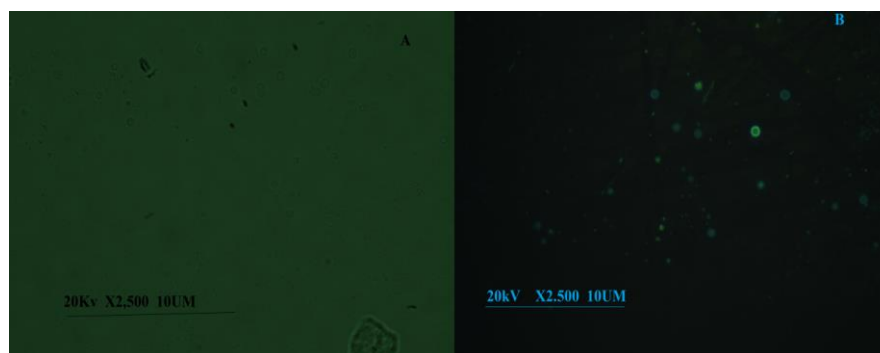


**Fig 7: HRTEM of CQDs FOURIER TRANSFORM INFRARED SPECTRUM OF COQDs**

## Results & Discussion

Fourier Transform Infrared (FTIR) spectra of the samples were obtained using a FTIR Jasco 4100 Spectrometer by KBr pellet method. The spectrums were recorded for the pure CQDs are shown in Fig.8 and its interpretation is given in Table 2

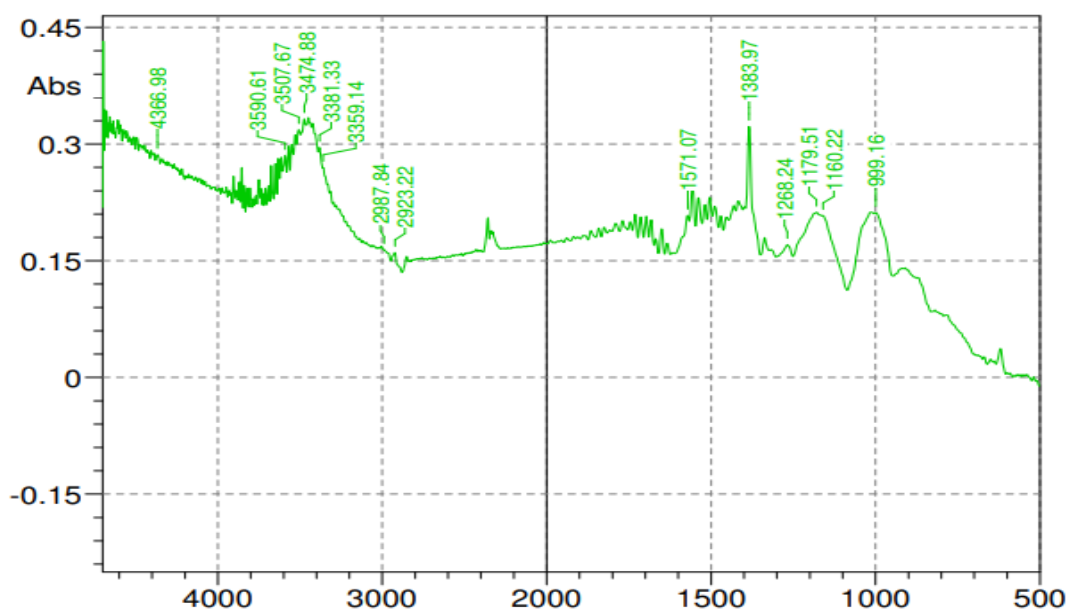


**Fig 8: FTIR spectrum of CQDs** Table 2. Interpretation of FTIR spectrum of prepared CQDS

Materials	Standard wave number (cm <sup>-1</sup> )	Test wave number (cm <sup>-1</sup> )	Functional group assignment
CQDS	1000-1420	1383.97	C-O or C-N and -COO asymmetric and symmetric stretching vibration
	1500-1680	1571.01	C=O stretching
	3650-3200	3474	O-H stretching, NH and carboxylic acid groups
	1161-1020	1160 1179-1268	In plane CH stretching

## Results & Discussion

---

The characteristic peak of C=O stretching vibration, which is a typical observation for CDs, is noticeable at  $1571\text{ cm}^{-1}$ . Also noticeable is the broad absorption band around  $3000\text{ cm}^{-1}$  which corresponds to the stretching of OH, NH, and carbocyclic acid functional groups; These functional groups typically exist on the surface of CDs<sup>[36]</sup>

### RAMAN SPECTRUM MEASUREMENT

Raman spectrum of CQDs are shown in Fig 8 and its interpretation is given in Table 3 and in Fig 9. Interpretation of Raman spectra further confirms the presence of C-C group and c-O group in the CQDs. Raman spectroscopy indicated that the CQDs had a relatively high degree of grahitization The disorder of D-band is related to defects in the graphite lattice (ie sp<sup>3</sup> carbon) and the G band is related to sp<sup>2</sup> hybridized carbon networks.<sup>[(37)]</sup>

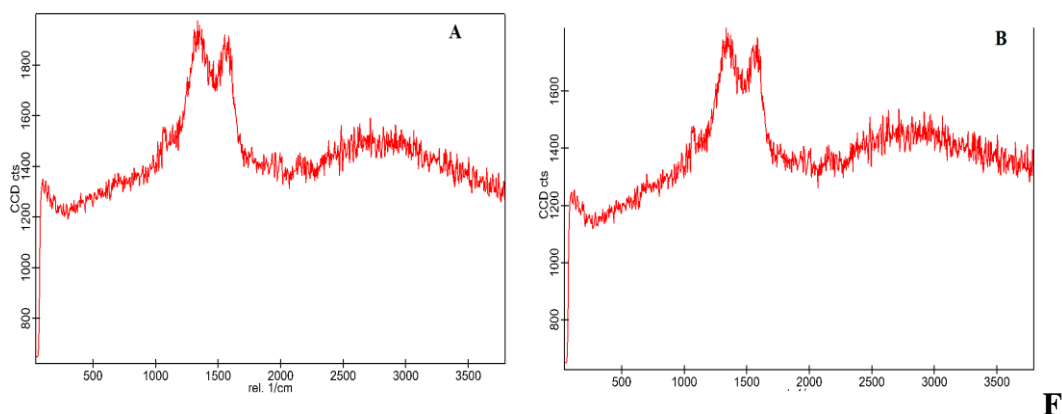


**Fig 9: Raman spectrum of CQDs Table 3. Interpretation of Mass spectrum of prepared CQDs**

## Results & Discussion

Materials	Standard wave number (cm <sup>-1</sup> )	Test wave number (cm <sup>-1</sup> )	Functional group assignment
COQDs	1000-1420	1390.88	D band (Disordered SP <sup>3</sup> hybridised Carbon)
	1600-1680	1618.51	G band (Ordered SP <sup>2</sup> hybridised Carbon)

### ELEMENTARY ANALYSIS

Elementary analysis samples were obtained using a Jasco 4100 elementary analyzer. The spectra recorded for the COQDs are shown in Fig. 10. Elemental analysis showed an elemental weight percent of 29.02% carbon and 70.98% nitrogen, which indicates that nitrogen has been successfully doped into the COQDs' structure.

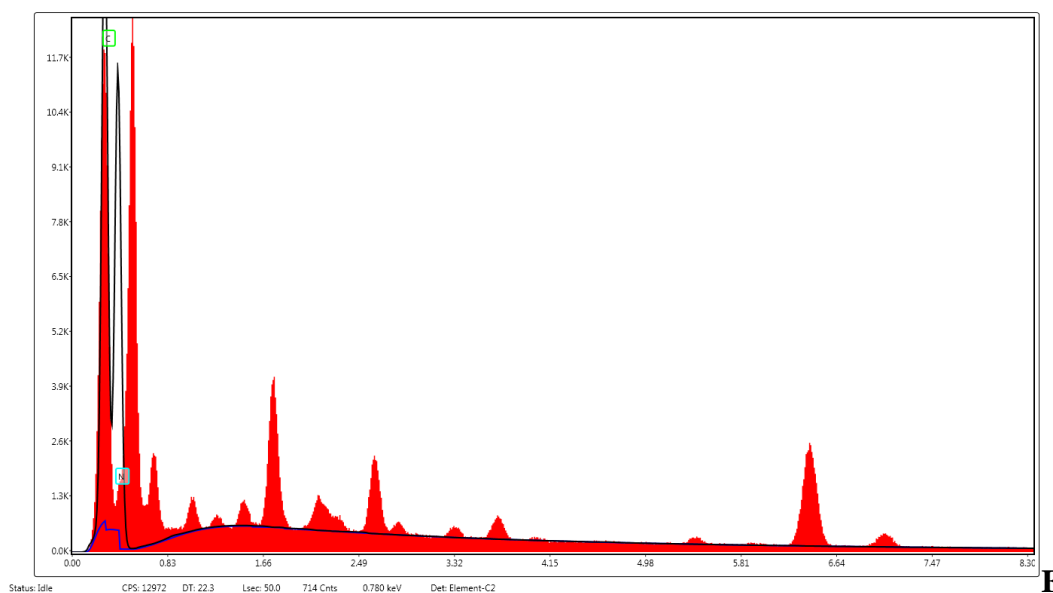


**Fig 10: Elementary analysis of prepared COQDs Table 4. Elementary of FTIR spectrum of prepared COQDs**

## Results & Discussion

Element	Weight %	Atomic %	Error %
C K	29.02	32.29	4.05
N K	70.98	67.71	9.43

### Confocal Fluorescence imaging

#### CQDs

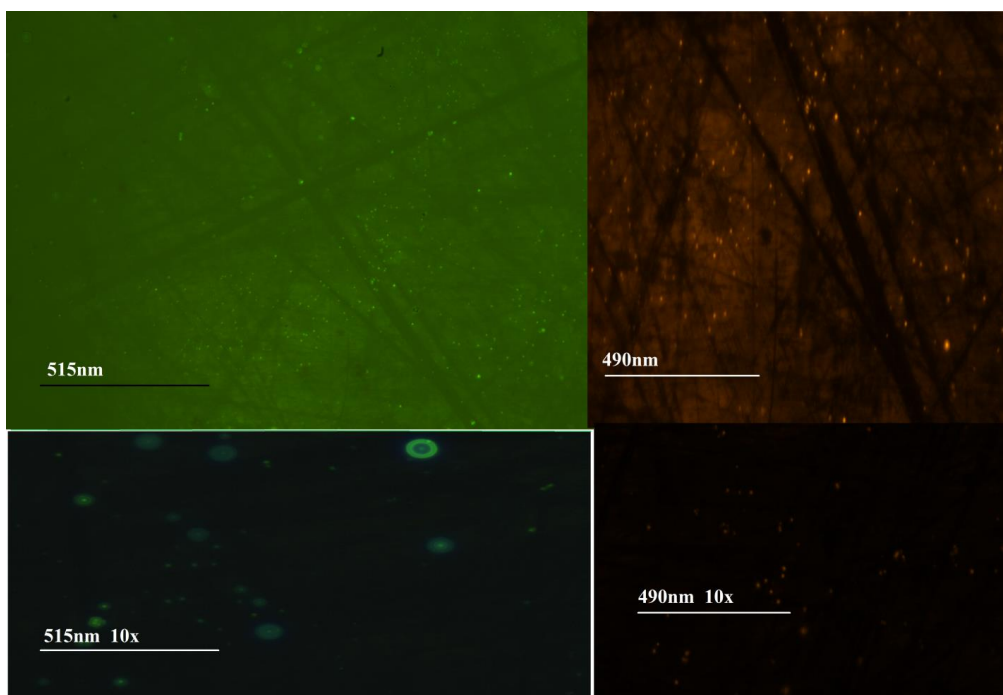


**Fig 11: Confocal fluorescence imaging of prepared CQDs**

The imaging process is done under confocal fluorescence microscope with laser excitation at 490 nm and 515nm, and fluorescence was collected in blue, green and gold region .REFORMULATION STUDIES Physical Characteristics Sorafinib was checked for its color, odor and texture. Sorafinib is white colored powder in appearance, odorless and amorphous in nature. **Solubility** Solubility test for Sorafinib was carried out in different solvents such as ethanol, water, dichloromethane and chloroform and results are given in Table: 5 .

## Results & Discussion

**Table 5. Solubility evaluation of Sorafinib**

Sl. No	Solvent	Soluble	Sparing Soluble	Insoluble
1.	Ethanol	✓	✓	-
2.	Dichloromethane	✓ □	-	-
3.	Chloroform	-	✓	-
4.	Water	-	-	-

Table 5 indicated that Sorafinib is insoluble in water and is soluble in ethanol and dichloromethane. **Selection of Wavelength of maximum absorption ( $\lambda_{max}$ )** The stock solution Sorafinib of concentration 100 $\mu$ g/mL was scanned in the range of 200-400nm for  $\lambda_{max}$  using double beam UV Spectrophotometer. The absorption peak obtained is shown in Fig. 12.

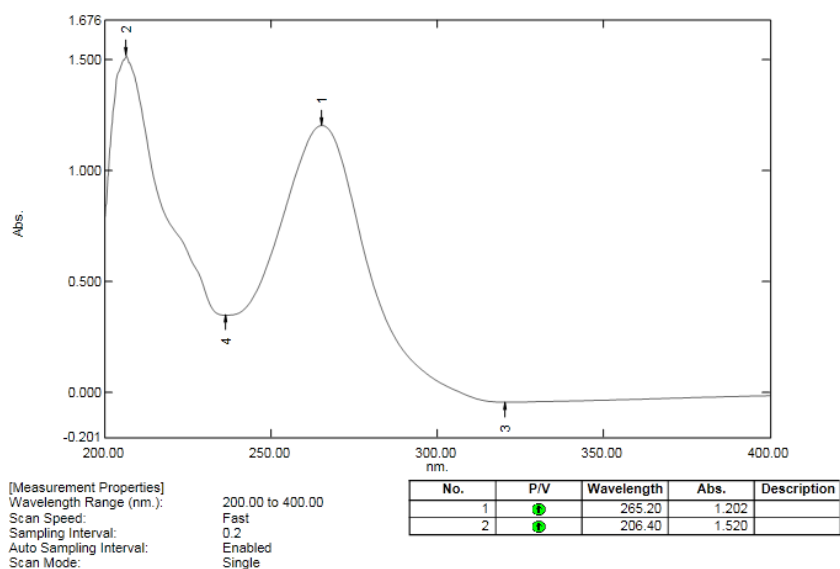


Fig. 2 Fig 12:

## Results & Discussion

### UV

**Visible spectrum of Sorfinib** The maximum absorption of sorafinib was found to be at 265nm and hence it is selected as the wavelength for further studies. Construction of calibration curve of sorafinib In the calibration curve, linearity was obtained between 5-40 µg/ml concentration of Sorafinib and the regression value was found to be  $r^2 = 0.9996$ . Hence we can conclude that Sorafinib obeys Beer Lambert's Law at the concentration between 5-40 µg/ml. The results are shown in Table 8 and Figure 13.

**Table: 6 Calibration concentration of Sorafinib**

Standard Table						
	Sample ID	Type	Ex	Conc	WL210.0	Wgt.Factor
1	a	Standard		0.000	0.000	1.000
2	b	Standard		10.000	0.193	1.000
3	c	Standard		20.000	0.352	1.000
4	d	Standard		30.000	0.486	1.000
5	e	Standard		40.000	0.633	1.000
6	f	Standard		50.000	0.767	1.000
7	g	Standard		60.000	0.879	1.000
8	h	Standard		70.000	1.019	1.000
9	i	Standard		80.000	1.177	1.000
10	k	Standard		90.000	1.366	1.000

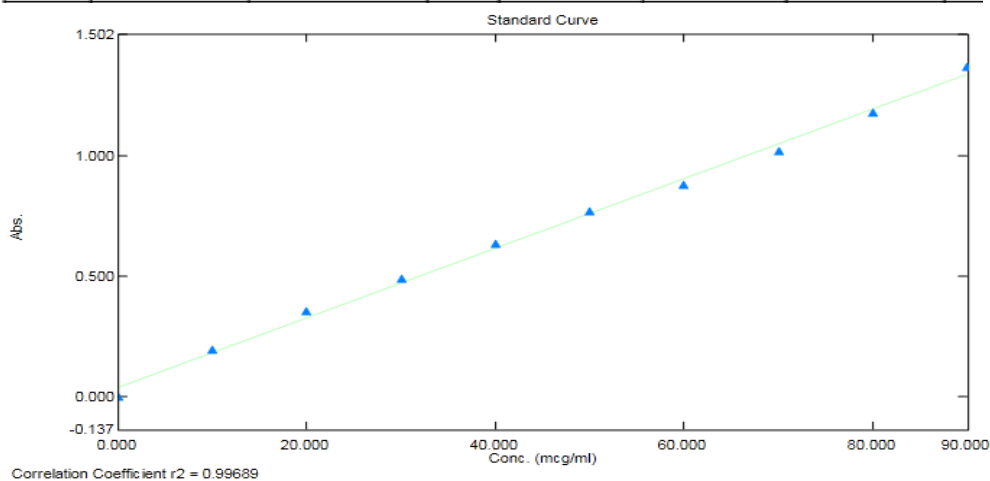


**Fig 13: Calibration curve of Sorfinib Formulation of Sorafinib COQ-Dot**

## Results & Discussion

---

### Conjugates.

The conjugated Sorafinib COQ-Dot conjugate was prepared in a trial and error basis method using Poly Ethylene Glycol (PEG) and Sodium tripolyphosphate as cross linking agents. The binding was better with the Sodium tripolyphosphate was selected for the study. Six formulations conjugated sorafinib CQDs (SF1 to SF6) were prepared with two different concentration of the binding agent TPP. The combinations of formulations are shown in Table 7.

**Table: 7 Formulation of sorafinib COQ-Dot Conjugates.**

Formulation code	Concentration of Sorafinib( $\mu\text{g/ml}$ )	Concentration of CQDs $\text{mM}$	Cross linking agent Sodium tripolyphosphate (%)
SF <sub>1</sub>	1000	90	5
SF <sub>2</sub>	1000	90	5
SF <sub>3</sub>	1000	90	5
SF <sub>4</sub>	500	100	10
SF <sub>5</sub>	500	100	10
SF <sub>6</sub>	500	100	10

### Drug loading

**Efficiency** the drug loading efficiency of sorafinib COQ-Dot conjugate were determined and is shown in Table 8. The SF1 to SF5 have encapsulation efficiency in the range of 67.24% to 84.1%. SF5 formulation has got the highest encapsulation efficiency. SF6 formulation has shown low encapsulation efficiency, So it has been removed from further studies.

**Table: 8 Encapsulation efficiency and Percentage yield of sorafinib COQ-Dot conjugate.**

## Results & Discussion

s.no	Formulation code	Sorafenib COQ-Dot conjugate cummulative (absorbance)	Percentage yield(%)
1	SF <sub>1</sub>	0.65±11.3	65.76±65.0
2	SF <sub>2</sub>	0.71±45.8	71.25±94.5
3	SF <sub>3</sub>	0.73±88.2	73.28±35.3
4	SF <sub>4</sub>	0.78±62.9	78.16±75.5
5	SF <sub>5</sub>	0.8±99.3	80.34±45.1
6	SF <sub>6</sub>	0.32±45.3	32.08±34.9

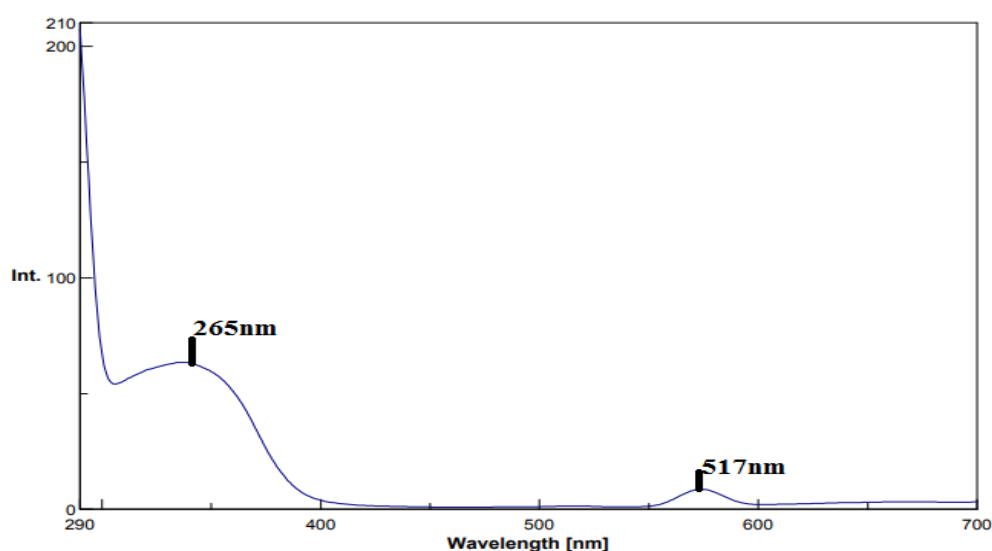


**Fig 14: UV Absorbance spectrum of formulated sorafenib COQ-Dot conjugate**

It is also possible that  $\pi$ - $\pi$  stacking between the phenyl ring of sorafenib and  $sp^2$  domain of the CDs could play a role in the binding. The absorbance peak of sorafenib appears at 345 nm, and the fluorescence peak of CQDs appears at 577 nm. Maxima does not appear to support an obvious fluorescence resonance energy transfer process from CQDs to Sorafenib CQD conjugate. We drew this conclusion from the changeless PL spectra before and after the CDs were

## Results & Discussion

Sorafenib conjugated CQD as shown in (Fig. 2 and Fig 14).

### Excipient Compatibility Studies:

Fourier Transform Infrared (FT-IR) spectra of the samples were obtained using a FTIR Jasco 4100 Spectrometer by KBr disc method. The spectrums were recorded for the pure drug, Sodium polyphosphate and sorafenib conjugate are shown in Figures 15, 16 and 17

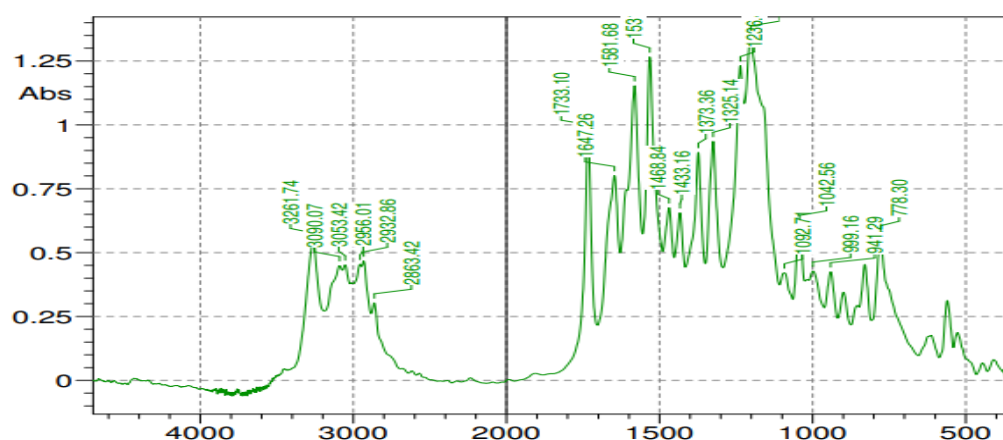
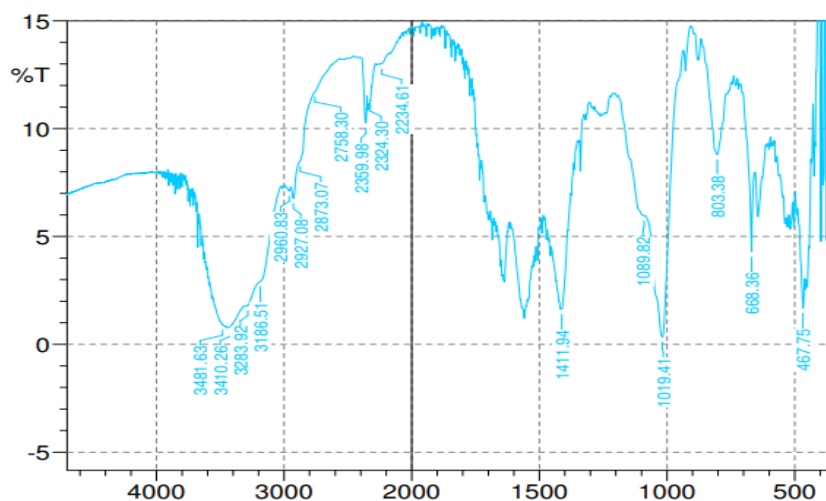


Fig :15 Sorafenib IR Spectrum Table:9 FTIR interpretation of sorafenib

Materials	Standard wave number (cm <sup>-1</sup> )	Testwave number (cm <sup>-1</sup> )	Functional group assignment
Sorafenib	1000-1420	1042.56	C-O or C-N and – COO asymmetric and symmetric stretching vibration
	1500-1680	1583.05	C=O stretching
	3650-3200	3261.75	O-H stretching, NH and carboxylic acid groups
	2761-2900	2863.4	C-O stretching

## Results & Discussion



**Fig:16 Cross linking agent TPP IR Spectrum**

**Table:10 FTIR interpretation of polymer**

Materials	Standard wave number (cm <sup>-1</sup> )	Test wave number (cm <sup>-1</sup> )	Functional group assignment
<b>Tripoly phosphoric acid</b>	3200-3650	3481.493625.52	OH stretching
	1485-1325	1411.75	C-O stretching

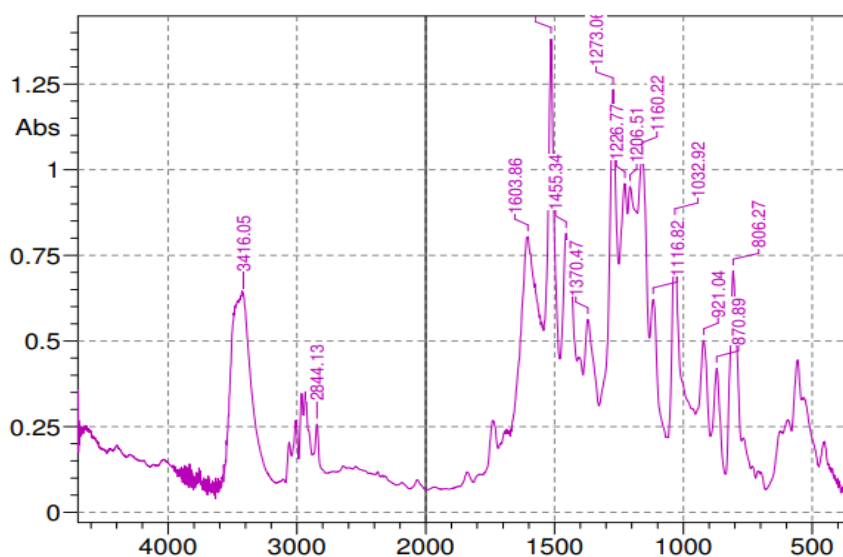


**Fig : 17 Formulation sorafinib COQ-Dot conjugate IR Spectrum**

## Results & Discussion

Table: 11 FTIR interpretation of sorafinib COQ-Dot conjugate

Materials	Standard wave number (cm <sup>-1</sup> )	Test wave number (cm <sup>-1</sup> )	Functional group assignment
Sorafinib COQ-Dot conjugate	1025-1045	1032	C-O or C-N and –COO asymmetric and symmetric stretching vibration
	1510-1650	1603	C=O stretching
	3200-3290	3416	O-H stretching, NH and carboxylic acid groups
	2761-2900	2844	C-O stretching

The prominent peaks of pure drug is available in Sorafinib CQD conjugate, So the Sorafinib, the cross linking agent Sodium tripolyphosphate and CQD are compatible. *In- vitro transport study* CQDs can be efficiently and rapidly excreted from the body after injection in different routes. Their blood clearance was quick-only 1 h post intravenous injection. The retention time is somewhat longer after subcutaneous and intramuscular injection. So the diffusion study was performed with many sampling for a period of 1 h.<sup>[38]</sup> The mean cumulative amount of drug release at each time point was calculated show in results Table 12 and Fig 18.

## Results & Discussion

**Table 12:** *In-vitro* drug release profile of sorafinib COQ-Dot conjugate (SF1-SF5)

Sl. No	Time(min)	Cumulative percentage drug release (%)				
		SF1	SF2	SF3	SF4	SF5
1	0	0	0	0	0	0
2	6	10.90	11.93	11.08	7.36	7.23
3	12	18.62	20.26	15.7	19.33	18.96
4	24	31.76	34.89	29.39	30.13	29.89
5	30	56.00	50.01	51.24	53.11	51.54
6	45	70.23	77.37	65.86	76.93	74.89
7	60	87.94	82.73	79.71	82.19	88.16

*In-vitro* release data of Sorafinib tablets in Table 8 indicated that the drug release is slowly increasing. Except F4, all the five formulations release above 80% of the drug in 1 h. Formulation F5 released the highest proportion of drug of all among all five formulations.

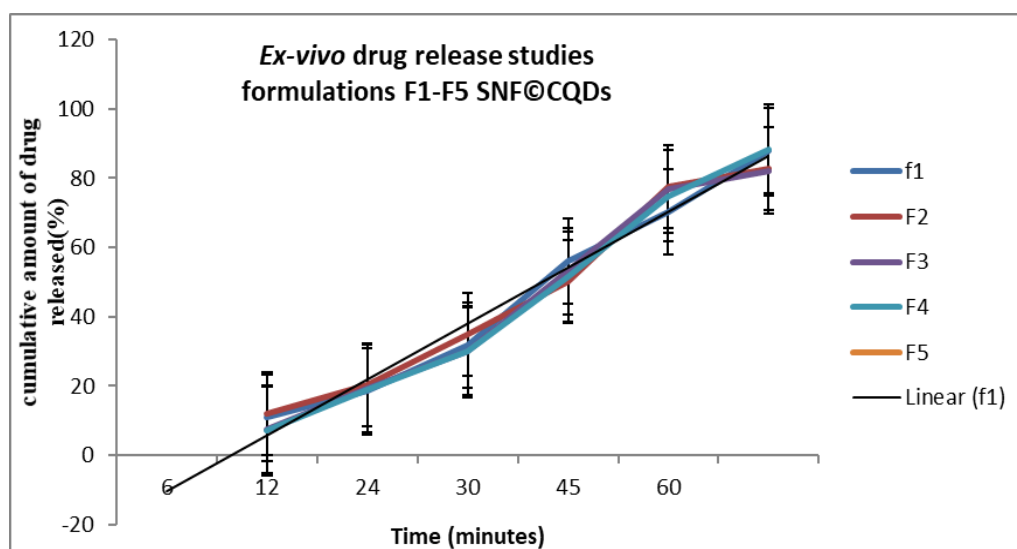


**Fig18:** *In vitro* drug release profile of sorafinib COQ-DotS formulations (F1-F5)

## Results & Discussion

### Cytotoxicity Studies

SH-SY5Y cell lines: SHS-Y5Y cell lines are human neuroblast cell from neural tissue and is used for the studies. Cytotoxicity studies showed that C-dots were exceptionally biocompatible on SH-SY5Y cell under ideal conditions of growth. Fig 19 summarizes impact of different concentrations on C-dots, free sorafinib, and sorafi@C-dots conjugate on SH-SY5Y cell lines in terms of percentage viability at various concentrations of test samples. Cdots were found to have negligible impact on SH-SY5H cells at all the concentrations Fig 20. More than 90% cells were found to be healthy after incubation with bare C-dots up to  $\sim 90 \text{ mg mL}^{-1}$ . Free sorafinib was found to be highly inimical than C-dots showing 79% cell viability at its highest concentration (1.2 mM). sorafi@C-dots conjugate was found to be extremely compatible with respect to bare sorafinib. SH-SY5Y cells showed 93% survival initially which got reduced to 84% at highest concentration having equal concentrations of sorafinib and C-dots as compared to free sorafinib. This may be due to low dose achieve high therapeutic action of from C-dots.

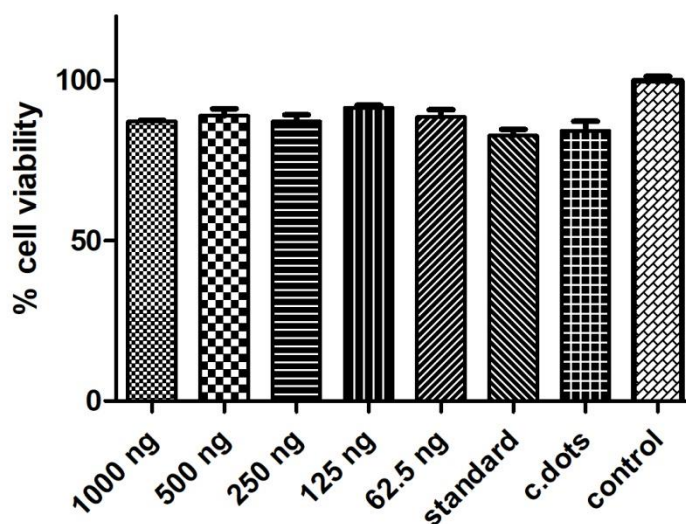


**Fig:19 Cytotoxicity of bare C-dots, bare sorafinib(Standard), and Sorafi@C-dots conjugate on SHSY5H cell lines**

## Results & Discussion

---

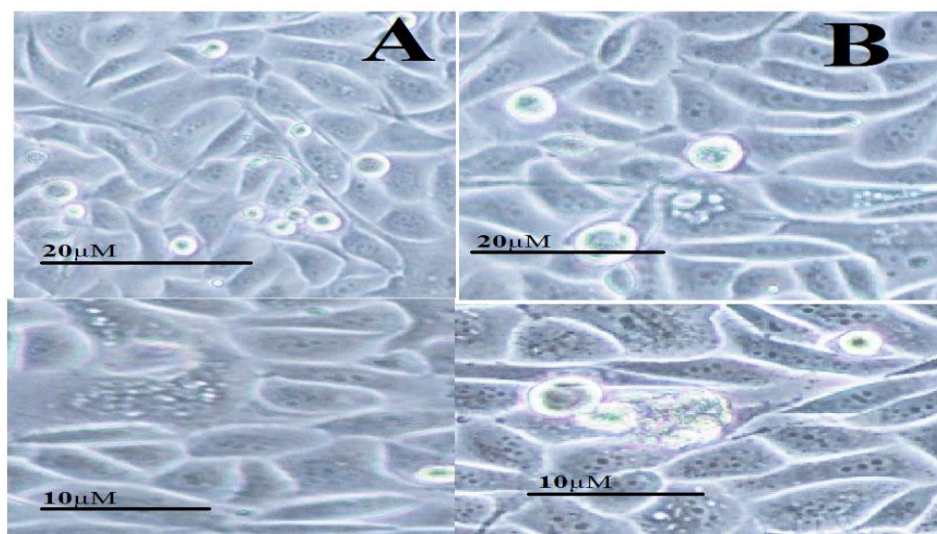


**Fig 20: Results from confocal fluorescence imaging (458 nm excitation) of (A) sorafenib (B) functionalized Sorafenib COQ-Dot conjugate carbon dots internalized SHSY5H in (incubation for 48 h).**

**MDA-MB 231 cell lines:** MDA-MB 231 cell lines is an epithelial human breast cancer cell, was used in the study. MDA MB 231 cell under ideal conditions of growth Fig : 20. summarizes impact of different concentrations on C-dots, free sorafenib, and sorafi@C-dots conjugate on shsy5h cell lines in terms of percentage viability at various concentrations of test samples. Cdots were found to have negligible impact on Mdamb231 cells at all the concentrations (Figure :20). More than 90% cells were found to be healthy after incubation with bare C-dots up to  $\sim 90 \text{ mg mL}^{-1}$ . Free sorafenib was found to be highly inimical than C-dots showing 84% cell viability at its highest concentration (1.4 mM). sorafi@C-dots conjugate was found to be extremely compatible with respect to bare sorafenib. Mdamb231 cells showed 93% survival initially which got reduced to 82% at highest concentration having equal concentrations of sorafenib and C-dots as compared to free sorafenib. This may be due to low dose achieve high therapeutic action of C-dots.

## Results & Discussion

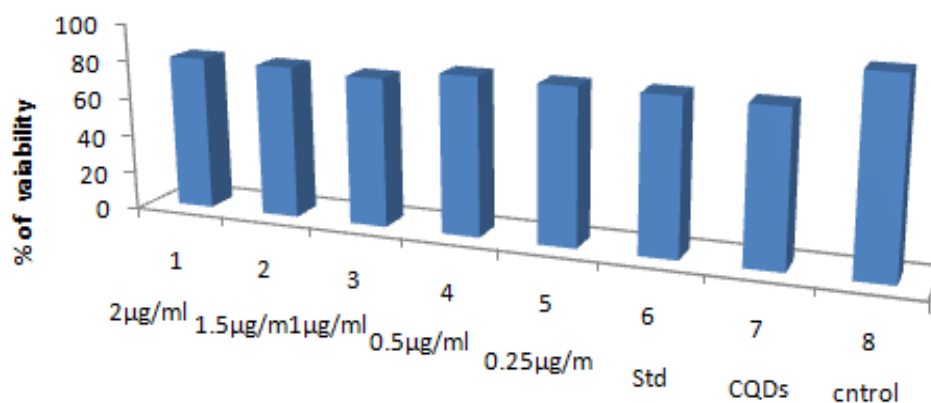


**Fig 21.** Cytotoxicity of bare C-dots, bare sorafinib(Standard), and Sorafi@C-dots conjugate on MDA-MB 231 cell lines.

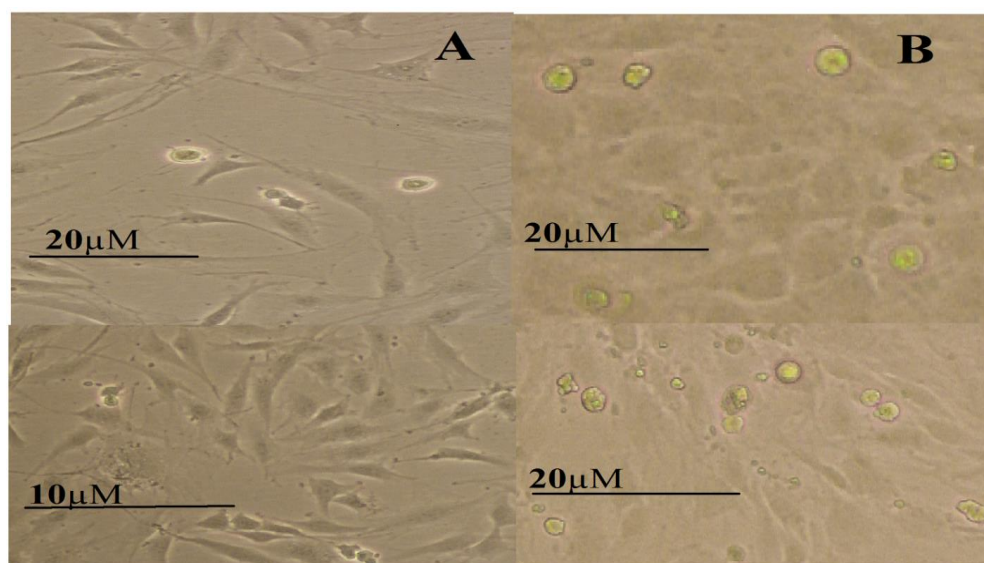


**Fig 22** Results from confocal fluorescence imaging (458 nm excitation) of (A) sorafinib (B) functionalized sorafinib COQ-Dot conjugate carbon dots internalized MDAMB231 in (incubation for 48 h)

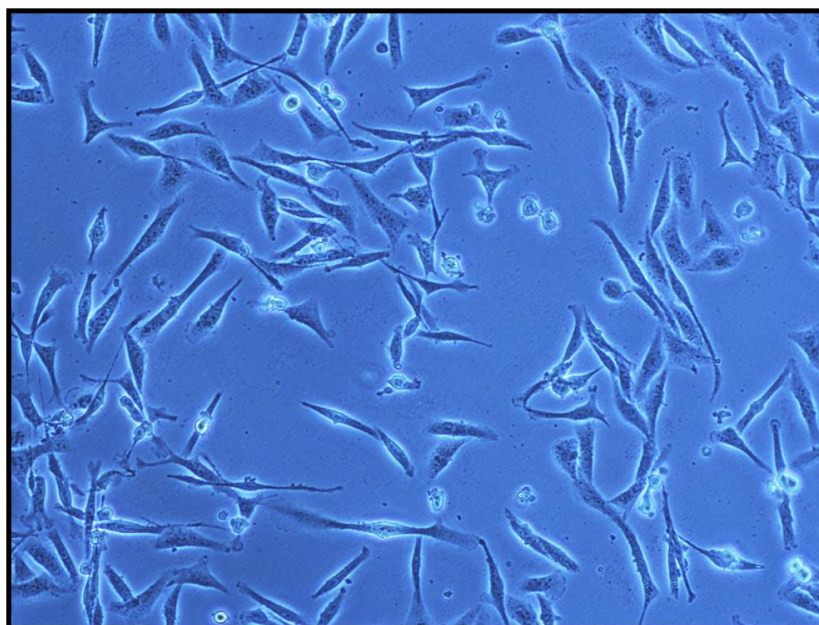


**Fig: 23** Results from confocal fluorescence imaging (458 nm excitation) of carbon dots internalized SHSY5H cells in (incubation for 48 h).

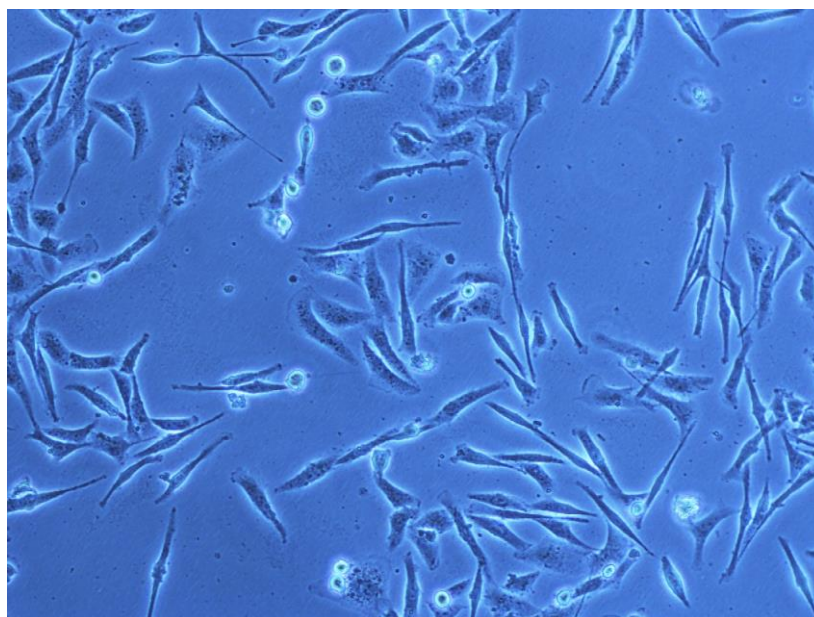


**Fig: 24** Results from confocal fluorescence imaging (458 nm excitation) of carbon dots internalized MDA MB 231 cells in (incubation for 48 h).

## Summary & Conclusion

---

### SUMMARY AND CONCLUSION

Cancer is becoming an increasingly important area of research and to this end carbon nanoparticle can serve as a powerful system for drug delivery. As these fields grow, carbon-based nanoparticles have been shown to be an effective means towards a drug delivery system in the effort to combat cancer. To this end, C-dots alongside similar carbon particles are nontoxic, unlike several other heavier, metal-based nanoparticles, and they possess functional groups similar in number and quantity to that of polymers like polyethylene glycol (PEG) commonly implemented in the field.

C-dots are becoming a prevalent platform for attachment of receptors alongside chemotherapy drugs due to the presence of rich surface functional groups (i.e., carboxylic and amino groups). In this study, Carbon Quantum Dots (CQD) have been synthesised with carbon precursor with the novel method by extraction with ethanol.

Synthesised CQDs showed excitation-dependent Photoluminescence, which is due to surface energy traps and the quantum effect. The quantum effect is related to particle size and causes blue emission. It was reported that excitation-dependent emission is due to different energy levels incorporated into the CQDs by different surface groups such as C-O, C=O, O=C-OH. P showed excitation-dependent passivation of the CQDs reduced the energy levels, and mono-color particles were produced. Main absorption band is obtained at 365 nm, with a yellow-pale orange color and blue fluorescent peak was obtained at 577nm. This photoluminescence property of CQDs paves the way of its usage in bio imaging applications.

Prepared CQDs were stable for more than two months while stored at 4 ° C with less than 5% loss in intensity, with quantum yield 25.6 %.

Synthesized CQDs are characterized by Malvern zeta sizer. Particle size analysis showed that the average particle size of CQDs was found to be

## Summary & Conclusion

---

27.53±9.45 nm and the particles are negatively charged with a zeta potential of -15.2. with peak area of 100% intensity. Having considered FTIR results, this negative charge is due to carboxylic groups on the surface. High zeta potential confirms a high degree of carboxylic functional groups.

HRTEM images showed that CQDs have smooth surface morphology with porous in nature and are spherical in shape. Fourier Transform Infrared (FTIR) spectra of the CQD indicated that the characteristic peak of C=O stretching vibration, which is a typical observation for CDs, is noticeable at 1571  $\text{cm}^{-1}$ . Also noticeable is the broad absorption band around 3000  $\text{cm}^{-1}$  which corresponds to the stretching of OH, NH, and carbocyclic acid functional groups; These functional groups typically exist on the surface of CQDs. Raman spectroscopy indicated that the CQDs had a relatively high degree of graphitization,

Elemental analysis showed elemental weight percent of 29.02% carbon and 70.98% nitrogen which shows that nitrogen is successfully doped into the CQDs' structure. The confocal microscopy images were also obtained.

Sorafenib is an anticancer drug used in the study. Sorafenib is white colored powder in appearance, odorless and amorphous in nature. Sorafenib is insoluble in water and is soluble in ethanol and dichloromethane.

The conjugated Sorafenib COQ-Dot conjugate was prepared in a trial and error asis method using Poly Ethylene Glycol (PEG) and Sodium tripolyphosphate as cross linking agents. The binding was better with the Sodium tripolyphosphate(TPP) was selected for the study. Six formulations conjugated sorafenib CQDs (SF1 to SF6) were prepared with two different concentration of the binding agent TPP. It is also possible that  $\pi$ - $\pi$  stacking between the phenyl ring of sorafenib and  $\text{sp}^2$  domain of the CDs could play a role in the binding.

The drug loading efficiency of sorafenib COQ-Dot conjugate were determined. In compatibility study, The prominent peaks in FTIR spectrums of

## Summary & Conclusion

---

pure drug is available in Sorafinib CQD conjugate, then sorafinib, the cross linking agent Sodium tripolyphosphate and CQD are compatible. The HRTEM images of formulations F4 and F6 are obtained .

*In -vitro* transport study was performed by diffusion cell method, diffusion cell having an area of 1.5cm, using specified (Phosphate buffer pH 6.8) as the receptor media. A small quantity of SNB-tablets (equivalent to 50mg of sorafinib COQ-Dot conjugate,) was placed on the egg yolk membrane surface, for a period of 1 h.*In-vitro* release data of Sorafinib tablets in Table 8 indicated that the drug release is slowly increasing. Except F4, all the five formulations release above 80% of the drug in 1 h. Formulation F5 released the highest proportion of drug of all among all six formulations.

Cell line studies were conducted. SHSY5Y cell lines are human neuroblast cell from neural tissue and is used for the studies. Cytotoxicity studies showed that C-dots were exceptionally biocompatible on SH-SY5Y cell under ideal conditions of growth More than 90% cells were found to be healthy after incubation with bare C-dots up to  $\sim 90 \text{ mg mL}^{-1}$ . Free sorafinib was found to be highly inimical than C-dots showing 79% cell viability at its highest concentration (1.2 mM). sorafi@C-dots conjugate was found to be extremely compatible with respect to bare sorafinib. shsy5h cells showed 93% survival initially which got reduced to 84% at highest concentration having equal concentrations of sorafinib and C-dots as compared to free sorafinib. This may be due to low dose achieve high therapeutic action of from C-dots. Cdots were found to have negligible impact on SH-SY5H cells at all the concentrations

MDA-MB 231 cell lines is an epithelial human breast cancer cell , was used in another cell line study. MDAMB231 cell under ideal conditions of growth ,more than 90% cells were found to be healthy after incubation with bare C-dots

## Summary & Conclusion

---

up to  $\sim 90 \text{ mg mL}^{-1}$ . Free sorafenib was found to be highly inimical than C-dots showing 84% cell viability at its highest concentration (1.4 mM). sorafenib CQDs conjugate was found to be extremely compatible with respect to bare sorafenib. Mdamb231 cells showed 93% survival initially which got reduced to 82% at highest concentration having equal concentrations of sorafenib and C-dots as compared to free sorafenib. This may be due to low dose achieve high therapeutic action of from CQDs.

### CONCLUSION

It was concluded that CQDs can be synthesized by a novel easy ethanol extraction method. using AM fruit powder as a candidate for natural carbon precursor. The synthetic protocol is green and fast. The surface state is studied by FTIR and Raman spectra evaluations, as well as optical properties, showed that the method of CQDs preparations effect on the final particles surfaces functional groups. This study investigated that synthesized CQDs from AM fruit has anticancer activity. And it's sorafenib conjugate has also possess anticancer activity. So this study will be a milestone in usage of low dose of drug achieve high therapeutic action from C-dots in cancer patients. So this synthesized carbon dot and its Sorafenib conjugate can be used as targeted trackable drug delivery for cancer treatment.

### BIBLIOGRAPHY

1. Nagamalai Vasimalai†1, Vânia Vilas-Boas†1,2, Juan Gallo1 , María de Fátima Cerqueira3 , Mario Menéndez-Miranda4 , José Manuel Costa-Fernández4 , Lorena Diéguez1 , Begoña Espiñal and María Teresa Fernández-Argüelles\*1 Beilstein J. Nanotechnol. 2018, 9, 530–544.
2. Zheng XT, Ananthanarayanan A, Luo KQ, Chen P. Glowing graphene quantum dots and carbon dots: properties, syntheses, and biological applications. *Small*. 2015;11(14):1620–1636. doi:10.1002/sml.201402648
3. Youfu Wang and Aiguo Hu. *J. Mater. Chem. C*, 2014, 2, 6921. DOI: 10.1039/c4tc00988f.
4. Sheela Modani, Meena Kharwade, Monika Nijhawan. *International Journal of Current Pharmaceutical Research* ISSN- 0975-7066 Vol 5, Issue 4, 2013
5. Zahra Ramezani, Maryam Qorbanpour, Nadereh Rahbar S0927-7757(18)30276-0 DOI: <https://doi.org/10.1016/j.colsurfa.2018.04.006>
6. Zhang X, Jiang M, Niu N, et al. Natural-Product-Derived Carbon Dots: From Natural Products to Functional Materials. *ChemSusChem*. 2018;11(1):11–24. doi:10.1002/cssc.201701847
7. Daniela Iannazzo, Alessandro Pistone, Consuelo Celesti, Claudia Triolo, Salvatore Patané, Salvatore V. Giofré, Roberto Romeo, Ida Ziccarelli, Raffaella Mancuso *Nanomaterials* 2019, 9, 282; doi:10.3390/nano9020282.
8. Joel Pardo, Zhili Peng, ID and Roger M. Leblanc 1, *Molecules* 2018, 23, 378; doi:10.3390/molecules23020378.
9. Joe Weaver, a Rashid Zakeri, a Samir Aouadib and Punit Kohli a *J. Mater. Chem.*, 2009, 19, 3198–3206.
10. Hui Ding, Yuan Ji, Ji-Shi Wei, Qing-Yu Gao, Zi-Yuan Zhou and Huan-Ming Xiong, DOI: 10.1039/c7tb01130j.

## Bibliography

---

11. Mukeshchand Thakur, Sunil Pandey, Ashmi Mewada, Vaibhav Patil, Monika Khade, Ekta Goshi, and Madhuri Sharon Journal of Drug Delivery Volume 2014, Article ID 282193, 9 pages <http://dx.doi.org/10.1155/2014/282193>.
12. Q. Zeng, D. Shao, X. He, Z. Ren, W. Ji, C. Shan, S. Qu, J. Li, L. Chen and Q. Li, J. Mater. Chem. B, 2016, DOI: 10.1039/C6TB01259K.
13. Masoud Farshbaf, Soodabeh Davaran, Fariborz Rahimi, Nasim Annabi, Roya Salehi & Abolfazl Akbarzadeh (2017): Carbon quantum dots: recent progresses on synthesis, surface modification and applications, Artificial Cells, Nanomedicine, and Biotechnology, DOI: 10.1080/21691401.2017.1377725.
14. Pardo J, Peng Z, Leblanc RM. Cancer Targeting and Drug Delivery Using Carbon-Based Quantum Dots and Nanotubes. *Molecules*. 2018;23(2):378. Published 2018 Feb 10. doi:10.3390/molecules23020378
15. Madani SY, Shabani F, Dwek MV, Seifalian AM. Conjugation of quantum dots on carbon nanotubes for medical diagnosis and treatment. *Int J Nanomedicine*. 2013;8:941–950. doi:10.2147/IJN.S36416
16. Mukerjee A, Ranjan AP, Vishwanatha JK. Combinatorial nanoparticles for cancer diagnosis and therapy. *Curr Med Chem*. 2012;19(22):3714–3721. doi:10.2174/092986712801661176
17. Zulfajri M, Gedda G, Chang CJ, Chang YP, Huang GG. Cranberry Beans Derived Carbon Dots as a Potential Fluorescence Sensor for Selective Detection of Fe<sup>3+</sup> Ions in Aqueous Solution. *ACS Omega*. 2019;4(13):15382–15392.
18. Kong T, Hao L, Wei Y, Cai X, Zhu B. Doxorubicin conjugated carbon dots as a drug delivery system for human breast cancer therapy. *Cell Prolif*. 2018;51(5):e12488. doi:10.1111/cpr.12488.
19. Wu F, Yue L, Su H, Wang K, Yang L, Zhu X. Carbon Dots @ Platinum Porphyrin Composite as Theranostic Nanoagent for Efficient Photodynamic Cancer Therapy [publishe.d correction appears in

## Bibliography

---

- Nanoscale Res Lett. 2019 Jan 9;14(1):16]. Nanoscale Res Lett. 2018;13(1):357. Published 2018 Nov 8. doi:10.1186/s11671-018-2761-5
20. Jiang X, Shi Y, Liu X, *et al.*, Synthesis of Nitrogen-Doped Lignin/DES Carbon Quantum Dots as a Fluorescent Probe for the Detection of Fe<sup>3+</sup> Ions. *Polymers (Basel)*. 2018;10(11):1282. Published 2018 Nov 17. doi:10.3390/polym10111282.
  21. Dager A, Uchida T, Maekawa T, Tachibana M. Synthesis and characterization of Mono-disperse Carbon Quantum Dots from Fennel Seeds: Photoluminescence analysis using Machine Learning. *Sci Rep*. 2019;9(1):14004. Published 2019 Sep 30. doi:10.1038/s41598-019-50397-
  22. Dias C, Vasimalai N, P Sárria M, *et al.* Biocompatibility and Bioimaging Potential of Fruit-Based Carbon Dots. *Nanomaterials (Basel)*. 2019;9(2):199. Published 2019 Feb 3. doi:10.3390/nano9020199.
  23. Zhang XD, Li J, Niu JN, Bao XP, Zhao HD, Tan M. Fluorescent carbon dots derived from urine and their application for bio-imaging. *Methods*. 2019;168:84–93. doi:10.1016/j.ymeth.2019.04.005
  24. Shi Y, Liu X, Wang M, *et al.* Synthesis of N-doped carbon quantum dots from bio-waste lignin for selective irons detection and cellular imaging. *Int J Biol Macromol*. 2019;128:537–545. doi:10.1016/j.ijbiomac.2019.01.146
  25. Bhatt S, Bhatt M, Kumar A, Vyas G, Gajaria T, Paul P. Green route for synthesis of multifunctional fluorescent carbon dots from Tulsi leaves and its application as Cr(VI) sensors, bio-imaging and patterning agents. *Colloids Surf B Biointerfaces*. 2018;167:126–133. doi:10.1016/j.colsurfb.2018.04.008
  26. Dong Y, Wan L, Cai J, Fang Q, Chi Y, Chen G. Natural carbon-based dots from humic substances. *Sci Rep*. 2015;5:10037. Published 2015 May 6. doi:10.1038/srep10037.
  27. Song J, Zhang J. Self-illumination of Carbon Dots by Bioluminescence Resonance Energy Transfer. *Sci Rep*. 2019;9(1):13796. Published 2019 Sep 24. doi:10.1038/s41598-019-50242-9.

## Bibliography

---

28. Zhao Y, Shi L, Fang J, Feng X. Bio-nanoplatfoms based on carbon dots conjugating with F-substituted nano-hydroxyapatite for cellular imaging. *Nanoscale*. 2015;7(47):20033–20041. doi:10.1039/c5nr06837a.
29. Kang YF, Li YH, Fang YW, Xu Y, Wei XM, Yin XB. Carbon Quantum Dots for Zebrafish Fluorescence Imaging. *Sci Rep*. 2015;5:11835. Published 2015 Jul 2. doi:10.1038/srep11835.
30. Molaei MJ. A review on nanostructured carbon quantum dots and their applications in biotechnology, sensors, and chemiluminescence. *Talanta*. 2019;196:456–478. doi:10.1016/j.talanta.2018.12.042.
31. Islam Rady, Melissa B. Bloch, Roxane-Cherille N. Chamcheu, Sergette Banang Mbeumi, Md Rafi Anwar, Hadir Mohamed, Babatunde, Jules-Roger Kuate, Felicite K. Noubissi, Khalid A. El Sayed, G. Kerr Whitfield, and Jean Christopher Chamcheu. *Oxid Med Cell Longev*. 2018; 2018: 1826170.
32. Zhao J, Liu C, Li Y, et al. Preparation of carbon quantum dots based high photostability luminescent membranes. *Luminescence*. 2017;32(4):625–630. doi:10.1002/bio.3230
33. Li K, Zhao X, Wei G, Su Z. Recent Advances in the Cancer Bioimaging with Graphene Quantum Dots. *Curr Med Chem*. 2018;25(25):2876–2893. doi:10.2174/0929867324666170223154145
34. Q. Tang, W. Zhu, B. He, P. Yang Rapid conversion from carbohydrates to large-scale carbon quantum dots for all-weather solar cells, *ACS Nano*, 11 (2017), p. 6b06867, *acsnano*,
35. X.-M. Wei, Y. Xu, Y.-H. Li, X.-B. Yin, X.-W. He Ultrafast synthesis of nitrogen-doped carbon dots via neutralization heat for bioimaging and ensing applications, *RSC Adv.*, 4 (2014), pp. 44504-44508, [CrossRefView Record in ScopusGoogle Scholar](#) ).
36. B.T. Hoan, P. Vanuan, H.N. Van, D.H. Nguyen, P.D. Tam, K.T. Nguyen, V.-H. Pham Luminescence of lemon-derived carbon quantum dot and its potential application in luminescent probe for detection of Mo6+ ions *Luminescence*, 33 (2018), pp. 545-551 )

## Bibliography

---

37. (37. V. Lee, L. Whittaker, C. Jaye, K.M. Baroudi, D.A. Fischer, S.Banerjee. “Large-Area Chemically Modified Graphene Films: Electrophoretic Deposition and Characterization by Soft X-ray,Absorption Spectroscopy”. Chem. Mater. 2009. 21(16): 3905-3916.
38. Mariadoss Asha Jhonsi, Carbon Quantum Dots for Bioimaging, ntechopen, 2018, doi:1.5772/intechopen.72723.



भारत सरकार  
GOVERNMENT OF INDIA  
पर्यावरण, वन और जलवायु परिवर्तन मंत्रालय  
MINISTRY OF ENVIRONMENT, FOREST & CLIMATE CHANGE  
भारतीय वनस्पति सर्वेक्षण  
BOTANICAL SURVEY OF INDIA



दक्षिणी क्षेत्रीय केन्द्र / Southern Regional Centre  
टी.एन.ए.यू. कैम्पस / T.N.A.U. Campus  
लाउली रोड / Lawley Road  
कोयंबटूर / Coimbatore - 641 003

टेलीफोन / Phone: 0422-2432788, 2432123  
टेलीफक्स / Telefax: 0422- 2432835  
ई-मेल / E-mail id: sc@bsi.gov.in  
bsisc@rediffmail.com

सं. भा.व.स./द.क्षे.के./No.: BSI/SRC/5/23/2020/Tech. /504

दिनांक/Date: 9<sup>th</sup> January 2020

**पौधे प्रमाणीकरण प्रमाणपत्र / PLANT AUTHENTICATION CERTIFICATE**

The plant specimen given by you for authentication is identified as *Annona muricata* L. - ANNONACEAE. The identified specimen is returned herewith for preservation in their College/ Department/ Institution Herbarium.

सेवा में / To

Mr. Mohammed Waseem A  
Semester IV (2<sup>nd</sup> Year) PG Student  
Department of Pharmaceutics  
Sri Ramakrishna Institute of Paramedical Sciences  
Coimbatore - 641 046

डॉ. सी. मुरुगन / Dr. C. Murugan  
वैज्ञानिक 'ई' एवं प्रभारी / Scientist 'E'-in-Charge  
वैज्ञानिक 'ई' एवं कार्यालय अध्यक्ष  
SCIENTIST 'E' & HEAD OF OFFICE - In-charge  
भारतीय वनस्पति सर्वेक्षण  
BOTANICAL SURVEY OF INDIA  
दक्षिणी क्षेत्रीय केन्द्र  
SOUTHERN REGIONAL CENTRE  
कोयंबटूर / COIMBATORE - 641 003

P. Murugan  
09/01/2020  
[P. MURUGAN]